

## RESEARCH ARTICLE

10.1029/2017MS001169

## Key Points:

- An optimality model incorporating ecohydrological theory can predict long-term average steady state leaf area index
- Terrestrial vegetation models could incorporate this approach to improve leaf area index predictions

## Supporting Information:

- Supporting Information S1
- Table S1

## Correspondence to:

J. Yang,  
jinyan.yang@westernsydney.edu.au

## Citation:

Yang, J., Medlyn, B. E., De Kauwe, M. G., & Duursma, R. A. (2018). Applying the concept of ecohydrological equilibrium to predict steady state leaf area index. *Journal of Advances in Modeling Earth Systems*, 10, 1740–1758. <https://doi.org/10.1029/2017MS001169>

Received 11 SEP 2017

Accepted 25 JUN 2018

Accepted article online 29 JUN 2018

Published online 3 AUG 2018

## Applying the Concept of Ecohydrological Equilibrium to Predict Steady State Leaf Area Index

J. Yang<sup>1</sup> , B. E. Medlyn<sup>1</sup> , M. G. De Kauwe<sup>2</sup> , and R. A. Duursma<sup>1</sup> 

<sup>1</sup>Hawkesbury Institute for the Environment, Western Sydney University, Sydney, New South Wales, Australia, <sup>2</sup>ARC Centre of Excellence for Climate Extremes, University of New South Wales, Sydney, New South Wales, Australia

**Abstract** Leaf area index (LAI) is a key variable in modeling terrestrial vegetation because it has a major impact on carbon and water fluxes. However, several recent intercomparisons have shown that modeled LAI differs significantly among models and between models and satellite-derived estimates. Empirical studies show that LAI is strongly related to precipitation. This observation is predicted by the ecohydrological equilibrium theory, which provides an alternative means to predict steady state LAI. We implemented this theory in a simple optimization model. We hypothesized that, when water availability is limited, plants should adjust steady state LAI and stomatal behavior to maximize net canopy carbon export, under the constraint that canopy transpiration is a fixed fraction of total precipitation. We evaluated the predicted LAI ( $L_{opt}$ ) for Australia against ground-based observations of LAI at 135 sites and continental-scale satellite-derived estimates. For the site-level data, the root-mean-square error of predicted  $L_{opt}$  was  $1.07 \text{ m}^2 \text{ m}^{-2}$ , similar to the root-mean-square error of a comparison of the data against 9-year mean satellite-derived LAI ( $L_{sat}$ ) at those sites. Continentally,  $L_{opt}$  had an  $R^2$  of 0.7 when compared to  $L_{sat}$ . The predicted  $L_{opt}$  increased continental-wide with rising atmospheric  $[\text{CO}_2]$  over 1982–2010, which agreed with satellite-derived estimations, while the predicted stomatal behavior responded differently in dry and wet regions. Our results indicate that long-term equilibrium LAI can be successfully predicted from a simple application of ecohydrological theory. We suggest that this theory could be usefully incorporated into terrestrial vegetation models to improve their predictions of LAI.

### 1. Introduction

Leaf area index (LAI; or  $L$  in equations) is a key biophysical variable in terrestrial biosphere models (TBMs), as it determines the exchange of carbon and water between the vegetation and the atmosphere. However, current TBMs systematically overestimate LAI when compared to satellite-derived estimates (Anav et al., 2013; Mahowald et al., 2016; Murray-Tortarolo et al., 2013). At individual sites, recent model intercomparisons have shown that there is a sizable spread among models ( $>4 \text{ m}^2 \text{ m}^{-2}$ ) in predicted maximum LAI (Medlyn et al., 2016; Walker et al., 2014). Models also disagree about the size of the projected change in LAI in response to warming and increasing atmospheric carbon dioxide ( $C_{at}$ ; De Kauwe et al., 2014; Mahowald et al., 2016). Typically, these models predict LAI as the outcome of leaf growth (dependent on net primary productivity, its allocation to leaves, and leaf mass per area) and turnover processes (usually constant input parameters). Uncertainty across models arises from differences in the way these processes are implemented, reflecting a lack of mechanistic understanding of the controls of these processes (De Kauwe et al., 2014).

An alternative approach that could be used to predict LAI is based on the idea of ecohydrological equilibrium: the LAI comes into equilibrium with the water availability at a given location (Eagleson, 1982). There is strong empirical support for a relationship between LAI and water availability especially in evergreen ecosystems. In *Eucalyptus*-dominated ecosystems in Australia, Specht and Specht (1989) found a strong ( $R^2 = 0.8$ ) relationship between LAI and an evaporative coefficient, represented as relative evapotranspiration/precipitation. Similarly, Ellis and Hatton (2008) reported a linear relationship between LAI and precipitation ( $R^2 = 0.8$ ) across eucalypt woodlands in southern Australia. Donohue et al. (2013) demonstrated a strong correlation between precipitation and satellite-derived maximum foliage coverage in dry regions of Australia. Across rainfall gradients of California, USA, Jin and Goulden (2014) analyzed precipitation and satellite-derived absorbed photosynthetically active radiation ( $Q_{APAR}$ ; generally assumed to be proportional to LAI) and found a saturating relationship with the sensitivity of  $Q_{APAR}$  to precipitation

©2018. The Authors.

This is an open access article under the terms of the Creative Commons Attribution-NonCommercial-NoDerivs License, which permits use and distribution in any medium, provided the original work is properly cited, the use is non-commercial and no modifications or adaptations are made.

being higher in drier regions. Globally, Iio et al. (2014) reported a strong LAI correlation with wetness index (precipitation/potential evapotranspiration [PET]) in dry regions, although the relationships varied with plant functional types ( $R$  varying from 0.13 to 0.57).

There have been relatively few attempts to incorporate this well-understood control on LAI into vegetation models. Woodward (1987) was the first to apply the idea of ecohydrological equilibrium in a large-scale model, predicting equilibrium LAI ( $L_{\text{equ}}$ ) from considerations of water and energy balance. In his approach, transpiration was calculated using the Penman-Monteith equation, in which increasing LAI was assumed to increase both canopy absorbed radiation and surface conductance.  $L_{\text{equ}}$  was given by the maximum value of LAI for which transpiration is less than incoming precipitation. Thus,  $L_{\text{equ}}$  maximized the absorbed radiation subject to the constraint of water availability. Since this calculation was based only on energy and water balance, it did not predict any change in  $L_{\text{equ}}$  with rising  $C_a$ .

Nemani and Running (1989) also used this theory to predict  $L_{\text{equ}}$  at stand scale. These authors used the FOREST-BGC model and empirical data to estimate the baseline transpiration and associated  $L_{\text{equ}}$  in one experimental pine stand in Montana, USA. They then modeled transpiration for 20 other similar stands and, by assuming the  $L_{\text{equ}}$ -transpiration relationship is constant, predicted  $L_{\text{equ}}$  for each stand. They found a strong correlation with the observed LAI ( $R^2 = 0.87$ ). However, this approach cannot be applied more broadly, since the relationship between transpiration and  $L_{\text{equ}}$  will vary with ecosystem type.

Kergoat (1998) suggested that a combination of water and carbon limitations would predict more realistic  $L_{\text{equ}}$  than consideration of water limitation alone and included two constraints on  $L_{\text{equ}}$ : (i) Plant transpiration (a function of both stomatal conductance [ $g_s$ ] and LAI) must not deplete soil moisture below a critical point, and (ii) the bottom layer of the canopy must have a positive carbon balance.  $L_{\text{equ}}$  was then predicted as the maximum LAI that satisfies these constraints. The predicted  $L_{\text{equ}}$  captured the LAI variation by biome globally, and the associated runoff matched observations in 28 sites. Kergoat (2002) expanded the model in Kergoat (1998) by additionally accounting for the construction cost of leaves and reported improved accuracy as compared to satellite-derived LAI. The approach proposed by Kergoat (2002) has not been widely adopted, possibly because of computational demands of a daily optimization.

Berling and Woodward (2001) incorporated  $L_{\text{equ}}$  as a component of Sheffield Dynamic Global Vegetation Model (SDGVM). The  $L_{\text{equ}}$  in SDGVM was based on similar carbon constraints as Kergoat (2002) but differed in the water balance constraint: They assumed that plant transpiration should be less than the precipitation reaching the ground. They also avoided the need to iterate by calculating LAI from the water and carbon balances of the previous year in a multiyear simulation. Woodward and Lomas (2004) validated the LAI predicted by SDGVM against optical measurements from the FLUXNET network and found a strong correlation ( $R^2 = 0.8$ ) across 52 sites. The  $L_{\text{equ}}$  model in SDGVM is more practical than the Kergoat models because of the simplification of water balance calculation. The goodness of fit of SDGVM  $L_{\text{equ}}$  to observations suggested that such a simplification may be reasonable and necessary considering the limitation in computational capacity. However, some recent applications of the SDGVM model have found it to significantly overestimate LAI at specific sites (De Kauwe et al., 2017; Medlyn et al., 2016).

One feature common to all the models described above is that the  $g_s$  response to drying soil is fixed. However, there is increasing empirical evidence to suggest that there are important differences in plant stomatal behavior across ecosystems and climatic zones (Lin et al., 2015). We take an alternative approach to predicting the ecohydrological equilibrium, based on the MATEY (Model Any Terrestrial Ecosystem–Yearly) model proposed by McMurtrie et al. (2008). In the original MATEY model, plants are assumed to maximize net carbon export by regulating both  $g_s$  and LAI, subject to the constraint that evapotranspiration cannot exceed a given fraction of incoming precipitation. The MATEY model thus optimizes both LAI and  $g_s$  at the same time. McMurtrie et al. (2008) evaluated their model at two forest stands but not on larger scales. We identified that a potential issue of optimizing both  $g_s$  and LAI is that the variabilities of  $g_s$  and LAI are on different temporal scales (minutes versus weeks). Hence, we characterized the variability of  $g_s$  using a model of stomatal behavior in which variation is represented by the stomatal slope parameter  $g_1$  (equation (S7) in the supporting information; Medlyn et al., 2011; Prentice et al., 2014). The term  $g_1$  is related to the water cost per unit carbon gain introduced by Cowan and Farquhar (1977) and is similar to the fitted slope in the widely used Ball-Berry model (Ball et al., 1987).

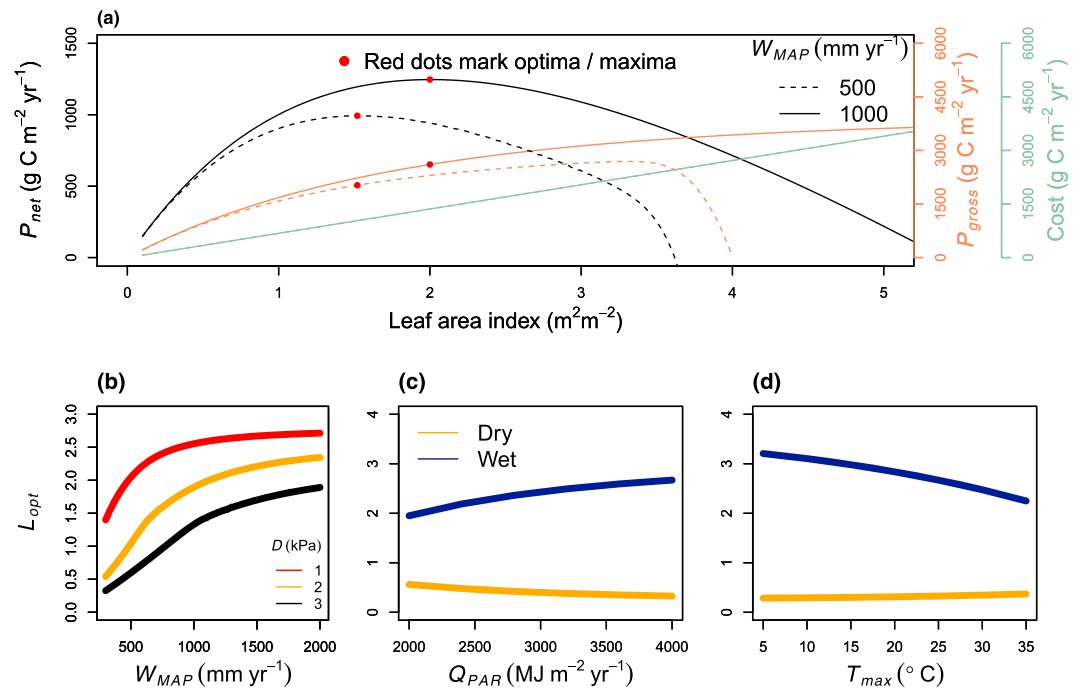


**Figure 1.** Model behavior and sensitivity. (a) Two examples of how model optima are obtained for two mean annual precipitation scenarios,  $W_{MAP}$  (500 and 1,000 mm); solid lines and dashed lines, respectively. Other inputs are set to  $D = 1.5$  kPa,  $Q_{PAR} = 3,000$   $\text{MJ PAR m}^{-2} \text{yr}^{-1}$ , and  $T_{max} = 25$   $^{\circ} \text{C}$ . The orange lines indicate gross primary production ( $P_{gross}$ , scale on right-hand axis); the green lines indicate foliage cost (scale on right-hand axis); the black lines indicate canopy net carbon export ( $P_{net}$ ), which equals  $P_{gross} - C_{total}$  (equation (7)). Sensitivity of predicted  $L_{opt}$  to climate factors for two scenarios: dry ( $W_{MAP} = 300$   $\text{mm yr}^{-1}$ ;  $D = 3$  kPa) and wet ( $W_{MAP} = 1,500$   $\text{mm yr}^{-1}$ ;  $D = 1$  kPa). (b) The relationship of  $L_{opt}$  to mean annual precipitation ( $W_{MAP}$ ) for three values of vapor pressure deficit ( $D$ ). Mean annual photosynthetically active radiation ( $Q_{PAR}$ ) and mean annual maximum temperature of each month ( $T_{max}$ ) were fixed to  $4,000$   $\text{MJ m}^{-2} \text{yr}^{-1}$  and  $25$   $^{\circ} \text{C}$ , respectively. (c and d) The impact of  $Q_{PAR}$  and  $T_{max}$  in conditions, respectively.

Here we investigate whether this optimality theory can successfully predict LAI across the Australian continent. Following McMurtrie et al. (2008) we take the approach of implementing the theory as simply as possible, applying a minimal set of equations to predict the long-term equilibrium. This approach allows us to focus on evaluating the performance of the theory independent of other model assumptions. Success of this simple parsimonious approach would indicate that the theory could usefully be incorporated into TBMs as an alternative to existing foliage carbon allocation schemes. We chose Australia as an example to evaluate the applicability of the concept of ecohydrological equilibrium because abundant and high-quality data are available for model construction (i.e., plant physiology and meteorology) and evaluation (i.e.,  $g_1$  and LAI data). In addition, Australia is dominated by evergreen ecosystems, for which the steady state approach is more easily interpreted. Utilizing the theory to predict LAI of deciduous ecosystems would require an additional set of assumptions regarding phenology (e.g., Caldararu et al., 2014).

The goal of this research is thus to explore the capacity of ecohydrological equilibrium theory to predict LAI at large scales. The outcome from this study should indicate whether incorporation of this theory is a potential avenue to improve the foliage carbon allocation schemes in existing TBMs. We tested several alternative implementations of the theory, identified the best-performing model, and evaluated the predictions against in situ data and satellite-derived estimates for Australia. To test its capacity to predict LAI in novel environmental conditions, we also used the model to predict the recent trend in LAI with the increase in atmospheric carbon dioxide and compared the predictions to satellite-derived observations.

## 2. Materials and Methods

### 2.1. Model

The model is a variant of the MATEY model (McMurtrie et al., 2008). It optimizes canopy net carbon export ( $P_{net}$ ;  $\text{g C m}^{-2} \text{yr}^{-1}$ ), the difference between canopy production and leaf construction and respiration

costs, for a given long-term climate, which is specified by the atmospheric CO<sub>2</sub> concentration ( $C_{ai}$ ;  $\mu\text{mol mol}^{-1}$ ), mean annual precipitation ( $W_{\text{MAP}}$ ;  $\text{mm yr}^{-1}$ ), vapor pressure deficit ( $D$ ; kPa), and annual total photosynthetically active radiation ( $Q_{\text{PAR}}$ ;  $\text{MJ PAR m}^{-2} \text{yr}^{-1}$ ).  $P_{\text{net}}$  is optimized based on a trade-off between LAI ( $\text{m}^2 \text{m}^{-2}$ ) and water use per unit leaf area, here represented by  $g_1$  ( $\text{kPa}^{0.5}$ ), the stomatal slope parameter (Medlyn et al., 2011). In the original MATEY model (McMurtrie et al., 2008), the optimization was a trade-off between LAI and stomatal conductance ( $g_s$ ;  $\text{mol H}_2\text{O m}^{-2} \text{s}^{-1}$ ). Here instead of using  $g_s$  directly, we model  $g_s$  as a function of the carbon assimilation rate,  $g_1$ ,  $D$ , and  $C_{ai}$ , with the optimal stomatal behavior model of Medlyn et al. (2011). We chose to use  $g_1$  because (i)  $g_1$  is related to plant water cost per unit carbon gain (Cowan & Farquhar, 1977; Medlyn et al., 2011) and thus combines the impacts of plant physiology, genetics, and prior environmental conditions; (ii)  $g_1$  is less temporally variable than  $g_s$  (Lin et al., 2015). A further difference from the original MATEY model is that our model considers the cost of foliage (both construction and maintenance), modeled as a function of LAI instead of being a fixed fraction of production (McMurtrie et al., 2008).

The trade-off between LAI and  $g_1$  in the model is represented by the responses of light use efficiency ( $\varepsilon_l$ ;  $\text{g C MJ}^{-1}$ ), water use efficiency ( $\varepsilon_w$ ;  $\text{g C mm}^{-1}$ ), the foliage cost per unit ground area ( $C_{\text{total}}$ ;  $\text{g C m}^{-2} \text{ground}$ ), and the absorbed photosynthetically active radiation ( $Q_{\text{APAR}}$ ;  $\text{MJ PAR m}^{-2} \text{yr}^{-1}$ ). Increasing LAI not only increases the fraction of absorbed  $Q_{\text{PAR}}$  and the transpiration fraction but also adds to  $C_{\text{total}}$ , while increasing  $g_1$  enhances  $\varepsilon_l$  but reduces  $\varepsilon_w$ . The total possible transpiration is set by  $W_{\text{MAP}}$  and the transpiration fraction, leading to a negative relationship between LAI and  $g_1$ . As a result, there are optimal values of LAI and  $g_1$  ( $L_{\text{opt}}$  and  $g_{1,\text{opt}}$ ) that maximize  $P_{\text{net}}$  under a given  $W_{\text{MAP}}$  (Figures 1 and 2). This  $L_{\text{opt}}$  is different from the  $L_{\text{equil}}$ , which is based on eco-hydrological equilibrium, by incorporating optimization. All symbols are defined at first use and again in Table S1 in the supporting information. Equations are defined in the following paragraphs and Text S1 in the supporting information. The model assumes the same equations and parameters for all plant functional types. Alternative assumptions were tested in developing the model (Appendix A) but showed little improvement of the prediction and were thus not incorporated for parsimony.

The water constraint in the model is represented by  $W_T$  (plant transpiration;  $\text{mm yr}^{-1}$ ), which was assumed to be a fraction of evapotranspiration following (Wang et al., 2014):

$$W_T = a_T \cdot L^{b_T} \cdot W_{\text{ET}} \quad (1)$$

where  $a_T$  and  $b_T$  are fitted parameters from Wang et al. (2014), with values of 0.77 and 0.1, respectively;  $L$  is LAI ( $\text{m}^2 \text{m}^{-2}$ ).  $W_{\text{ET}}$  is evapotranspiration ( $\text{mm yr}^{-1}$ ), which is related to mean annual precipitation following Zhang et al. (2001):

$$W_{\text{ET}} = \frac{W_{\text{MAP}} + 2 \cdot c_w}{1 + \frac{2 \cdot c_w}{W_{\text{MAP}}} + \frac{W_{\text{MAP}}}{c_w}} \quad (2)$$

where  $W_{\text{MAP}}$  is the mean annual precipitation ( $\text{mm yr}^{-1}$ ) and  $c_w$  is an empirical constant (fitted PET) in Zhang et al. (2001), with data for forest ecosystems. Our model here differs from McMurtrie et al. (2008), who assumed that a constant fraction (0.8) of rainfall was used by the plant. We used the more complicated calculation of transpiration because (i) transpiration can be less than half of total evapotranspiration (Kool et al., 2014; Sutanto et al., 2012; Wang et al., 2010; Wang & Dickinson, 2012; Yopez et al., 2005) (ii) and the fraction of transpiration in evapotranspiration is related to vegetation cover (Liu et al., 2017). The impacts of using these functions on the prediction are shown in Appendix A1.

The canopy carbon uptake is related to transpiration by the water use efficiency:

$$P_{\text{gross}} = \varepsilon_w \cdot W_T \quad (3)$$

where  $P_{\text{gross}}$  is gross primary production ( $\text{g C m}^{-2} \text{yr}^{-1}$ );  $\varepsilon_w$  is the transpiration efficiency ( $\text{g C kg}^{-1}$ ), calculated following Medlyn et al. (2011; equation (S1)).  $P_{\text{gross}}$  calculated with water limitation has to equal to that calculated with absorbed radiation:

$$P_{\text{gross}} = \varepsilon_l \cdot Q_{\text{APAR}} \quad (4)$$

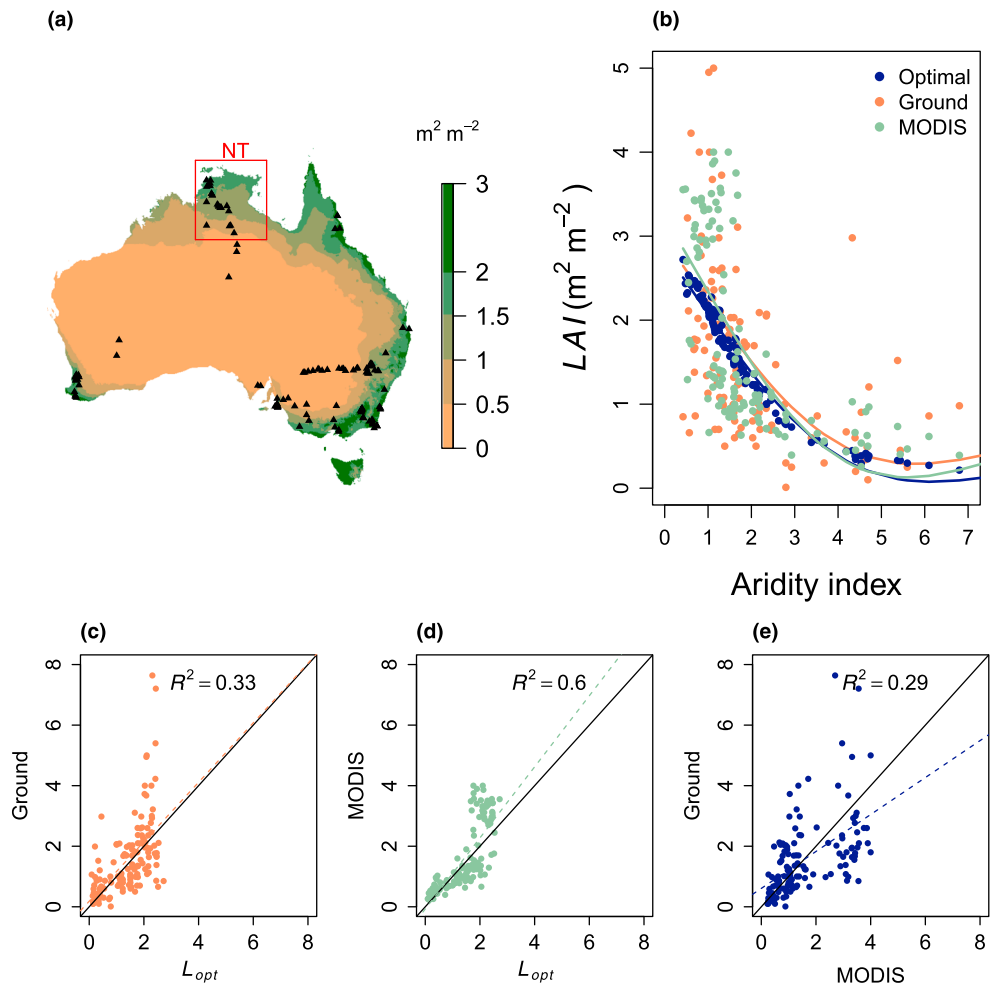


**Figure 2.** Optimal equilibrium leaf area index (LAI;  $L_{opt}$ ) plotted against AI (aridity index; potential evapotranspiration over mean annual precipitation). (a)  $L_{opt}$  for Australia, with site locations marked by triangles. The red square marks Northern Territory region discussed in section 3.3 and shown in Figure 4. (b) The mean of optimal, ground, and Moderate Resolution Imaging Spectroradiometer (MODIS) LAI of each site ( $n = 135$ ) plotted against AI. The smooth lines are generalized additive model fits. Linear regressions are shown for (c) ground versus  $L_{opt}$ , (d) MODIS versus  $L_{opt}$ , and (e) ground versus MODIS with  $R^2$ . The 1:1 line is shown by a solid line, while the colored, dashed lines are regression fits.

where  $\epsilon_j$  is light use efficiency ( $\text{g C MJ}^{-1} \text{ PAR}$ ), estimated with the model of Sands (1995, 1996; equations (S2)–(S7)), and  $Q_{APAR}$  (absorbed photosynthetically active radiation;  $\text{MJ PAR m}^{-2} \text{ yr}^{-1}$ ) of the canopy is related to LAI by the Beer-Lambert law (equation (S8)). This  $Q_{APAR}$  is the long-term average value: The model does not consider interannual and intraannual variation of climate conditions or of LAI. The responses of  $\epsilon_j$  to  $T_{max}$  and  $D$  are described in equations (S4)–(S6) following Bernacchi et al. (2001), Medlyn et al. (2002), Medlyn et al. (2007), and Medlyn et al. (2011).

Equations (3) and (4) are the key equations describing the water and light constraints in the model and the trade-off between  $g_1$  and LAI. Combining equations (3) and (4),  $g_1$  can be solved as a function of LAI. As a result,  $P_{gross}$  can be calculated as an implicit function of LAI, which is solved by iteration. The carbon cost of building leaves is given by  $C_{total}$ , which includes the maintenance respiration, construction respiration, and construction cost per unit ground area ( $\text{g C m}^{-2} \text{ yr}^{-1}$ ), defined as a function of LAI:

$$C_{total} = c_r \cdot R_m \cdot L + C_{cost} \cdot L \quad (5)$$

where  $c_r$  converts  $\mu\text{mol C m}^{-2} \text{ s}^{-1}$  to  $\text{g C m}^{-2} \text{ yr}^{-1}$ ;  $R_m$  is maintenance respiration per unit leaf area ( $\mu\text{mol m}^{-2} \text{ s}^{-1}$ );  $C_{cost}$  is the carbon cost of construction, including construction respiration per unit leaf

area ( $\text{g C m}^{-2}$  leaf). To estimate  $R_m$ , we used the Australian subset of the GLOBRESP data set (Atkin et al., 2015) and took the mean across available data. We assumed that the rate of respiration acclimates to the prevailing mean temperature and thus the value for  $R_m$  is taken to be a constant. We also considered two alternative assumptions for  $R_m$ , namely, a relationship with  $W_{\text{MAP}}$  or a relationship with leaf mass per area. The effects of these alternative assumptions are shown in Appendices A2 and A3.

The construction cost,  $C_{\text{cost}}$ , is calculated as

$$C_{\text{cost}} = c_c \cdot b_c \cdot \frac{M_{\text{area}}}{t_f} \quad (6)$$

where  $c_c$  is the assumed proportion of carbon in dry mass ( $0.5 \text{ g C g}^{-1} \text{ DM}$ ) and  $b_c$  is the construction respiration ratio ( $\text{g C g}^{-1} \text{ C}$ ). Villar and Merino (2001) reported a mean cost of 1.66 g of glucose per gram of dry mass for xeric forest. Assuming half of the dry mass is carbon and 40% of the glucose is carbon, we calculated the fraction of construction respiration ( $b_c$ ) to be  $1.3 \text{ (g C g}^{-1} \text{ C)}$ .  $M_{\text{area}}$  is leaf mass per area ( $\text{g DM m}^{-2}$  leaf), and  $t_f$  is the leaf lifespan (year). The values of  $M_{\text{area}}$  and  $t_f$  were taken as the mean from the GLOPNET data set (Wright et al., 2004; values are given in Table S1).

The model also relies on  $J_{\text{max}}$ , the maximum electron transport rate. We compiled a data set of Australian observations from the literature (Ali et al., 2015; De Kauwe et al., 2016; Walker et al., 2014; data available in Table S5) and tested for relationships with climate.  $J_{\text{max}}$  was not correlated with any climate factor used in the model (Figure S1 in the supporting information). Thus, we used the mean of the measurements from the data set. Similar to  $R_m$ , the temperature dependence of  $J_{\text{max}}$  is not included in the model.

The optimization target of the model, canopy net carbon export ( $P_{\text{net}}$ ;  $\text{g C m}^{-2} \text{ yr}^{-1}$ ), is then defined as the difference between production and cost:

$$P_{\text{net}} = P_{\text{gross}} - C_{\text{total}} \quad (7)$$

## 2.2. Data

The model was applied to predict  $L_{\text{opt}}$  and  $g_{1,\text{opt}}$  using gridded climate data and was evaluated against ground-based measurements (stand level) as well as satellite-derived estimates (0.06-degree grid).  $L_{\text{opt}}$  and  $g_{1,\text{opt}}$  were evaluated together for 10 sites where both measurements were available. To minimize anthropogenic effects, evaluation of the model at the continental scale was constrained to natural reserves.

### 2.2.1. Climate Inputs

Potential evapotranspiration ( $\text{mm yr}^{-1}$ ),  $W_{\text{MAP}}$ , actual vapor pressure,  $Q_{\text{PAR}}$ , and  $T_{\text{max}}$  are obtained from Ecosystem Modeling and Scaling Infrastructure (Whitley et al., 2014). We selected a 21-year period, 1991–2011, matching the satellite record (2000–2011). For computational efficiency, the climate data ( $0.01^\circ$  native resolution) were aggregated to  $0.06^\circ$ .  $D$  was calculated as the difference of saturation vapor pressure and actual vapor pressure with the former being a function of  $T_{\text{max}}$ . We also calculated an aridity index (AI), defined as  $\text{PET}/W_{\text{MAP}}$ . All the other gridded data sets in the following sections were aggregated to match the climate grids ( $0.06^\circ$ ). We used the long-term (21-year) mean of the four inputs for each grid cell. Plots of  $W_{\text{MAP}}$ ,  $D$ ,  $Q_{\text{PAR}}$ , and  $T_{\text{max}}$  are shown in Figure S2. The model predicted a paired  $L_{\text{opt}}$  and  $g_{1,\text{opt}}$  for each grid cell with no temporal variation.

### 2.2.2. Ground-Based Data

Ground-based LAI and  $g_1$  data were used for evaluation. Ground-based LAI measurements were taken from six sources: Ellis & Hatton (2008; 37 sites), Zeppel et al. (2008; one site), Mitchell et al. (2009; one site), Iio et al. (2014; 134 sites), Duursma et al. (2016; one site), and eight sites from the Terrestrial Ecosystem Research Network (TERN; Beringer & McHugh, 2015a, 2015b; Bradford, 2015; Eamus & Cleverly, 2015a, 2015b; Liddell & Laurance, 2015; Prober & Macfarlane, 2013; Prober & Macfarlane, 2015; Rowlings & Grace, 2015; van Gorsel, 2015). For sites that are close together ( $<0.01^\circ$ ), the mean of the reported LAI values was taken, giving a total of 135 sites. Both Duursma et al. (2016) and the data from TERN used the estimated gap fraction to estimate the LAI of the canopy. As a result, both data sets are plant area index. The data from Ellis and Hatton (2008) were a synthesis and thus the methods used to estimate LAI varied by source. Iio et al. (2014) synthesized a similar data set with various methods to estimate LAI but reported ecosystem LAI (sum of understory and canopy) instead of canopy when possible. Notably, the understory LAI could be as

high as canopy, and thus, these LAI measurements were likely underestimates. There are some notable inconsistencies among sources regarding their methodology: plant versus LAI, different methods to correct leaf clumping, and canopy versus ecosystem LAI. Moreover, the measurements are on stand level and are not scaled to the spatial resolution of satellite-derivatives and the modeled LAI. These LAI data were mostly one-time measurements and thus could not represent intraannual and interannual LAI variations. Corresponding ground-based  $g_1$  values were estimated from in situ leaf gas exchange measurements at the top of the canopy (Cernusak et al., 2011; Gimeno et al., 2016; Kelly, 2013; Medlyn et al., 2007; Mitchell et al., 2009; Zeppel et al., 2008), which were available for 10 of these sites (Table S4). Values were estimated from data using the “fitBB” routine (R package “plantecophys”; Duursma, 2015), which uses the nonlinear least squares method to fit  $g_1$  to measurements of stomatal conductance, photosynthesis, and environmental variables.

### 2.2.3. Satellite-Derived LAI Data

To evaluate the model’s performance at large spatiotemporal scales, we used the satellite-derived LAI product, MODIS (Moderate Resolution Imaging Spectroradiometer; Knyazikhin et al., 1999). The 8-day MODIS LAI (collection 5; MOD15A2) tiles for Australia were mosaicked and reprojected from their native sinusoidal projection to a regular latitude-longitude grid (GDA94; see Paget & King, 2008). The LAI estimates were averaged for the period 2000 to 2011. Only LAI data estimated from the main radiative transfer algorithm and deemed to be of the best quality (i.e., no cloud contamination or saturation data used; quality assurance flag = 0) were used.

### 2.2.4. Land Cover, Soil Attribute, and Digital Elevation Maps

The model used land cover type information taken from Australian Bureau of Agricultural and Resource Economics and Sciences product, National scale land use version 4 (2005–2006; <http://www.agriculture.gov.au/abares/aclump/Pages/land-use/data-download.aspx>). The soil attribute maps with total nitrogen ( $N_{\text{soil}}$ ; %) and phosphorus ( $P_{\text{soil}}$ ; %) of the top layer (0–5 cm) were obtained from CSIRO (Viscarra Rossel et al., 2014a, 2014b). The  $N_{\text{soil}}$  and  $P_{\text{soil}}$  data represented the total N and P in the soil and were aggregated from a native resolution (0.00083°) to 0.06°. The soil attributes were used for the statistical analysis of the importance of soil nutrients for LAI. We used the digital elevation model version 3 and flow direction grid 2008 obtained from Geoscience Australia (<http://www.ga.gov.au/metadata-gateway/metadata/record/66006/>).

### 2.2.5. Statistical Benchmark and Model Evaluation

We derived a statistical bench mark (Abramowitz, 2005) for the model by a generalized additive model (GAM) fitting LAI measurements as a function of climate. The fitting used a cubic spline basis with no interaction. This benchmarking is important because it quantifies the explanatory power of climate for LAI. We compared the model performance to this bench mark in order to determine how much of the information contained in the inputs is captured by the model.

We evaluated the model first at site level with measurements of both LAI and  $g_1$ . Then, we compared predicted  $L_{\text{opt}}$  to satellite derivatives at the scale of the whole continent, and for a sample region in the Northern Territory where there is a natural rainfall gradient spanning ~1,700 to ~300 mm ( $1 \text{ mm km}^{-1}$ ; Cernusak et al., 2011). The predictions should be linearly related to the observations if the model captures the key processes. Assessment of observed increase of LAI in response to rising  $C_a$  was done using Advanced Very High Resolution Radiometer NDVI (1982–2010; cf. Donohue et al., 2013). We applied the model to predict the response of  $L_{\text{opt}}$  and  $g_{1,\text{opt}}$  to this increase in  $C_a$  (holding long-term mean climate constant) and evaluated the predicted response of  $L_{\text{opt}}$  against these observations.

## 3. Results

### 3.1. $L_{\text{opt}}$ Sensitivity to Climate

Predicted  $L_{\text{opt}}$  was driven primarily by  $W_{\text{MAP}}$  and  $D$ , with  $Q_{\text{PAR}}$  and  $T_{\text{max}}$  modifying the results to a lesser extent. The impact of  $W_{\text{MAP}}$  was explained by the fact that the rainfall gradient (more than 20-fold) across Australia is much larger than that of  $D$ ,  $Q_{\text{PAR}}$ , or  $T_{\text{max}}$  (see Figure S2). The influence of  $D$  is the result of the sensitivity of light use efficiency to  $D$ . Assuming fixed  $D$ ,  $Q_{\text{PAR}}$ , and  $T_{\text{max}}$ , and at a given  $W_{\text{MAP}}$ ,  $P_{\text{gross}}$  showed a humped relationship with LAI due to the trade-off with  $g_1$ ; the peak occurred much earlier at lower  $W_{\text{MAP}}$  (orange lines in Figure 1a). Cost increases linearly with increasing LAI and does not vary with  $W_{\text{MAP}}$  (green line in Figure 1a). The optimum  $P_{\text{net}}$  is reached when the difference between  $P_{\text{gross}}$  and cost is maximized (shown as red dots). The predicted sensitivity (slope) of  $L_{\text{opt}}$  to  $W_{\text{MAP}}$  was stronger at low  $W_{\text{MAP}}$  and at low  $D$ , both of

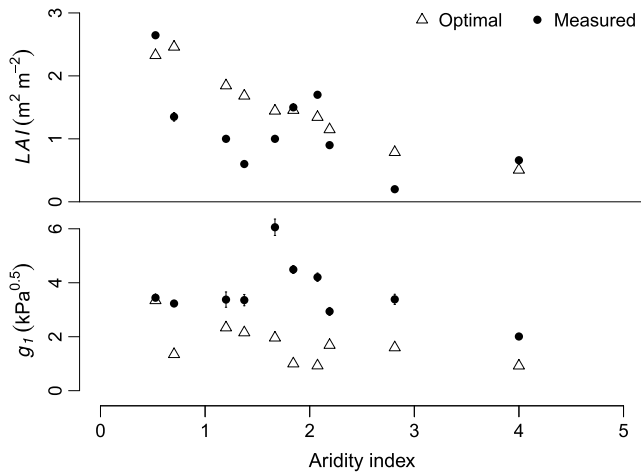


**Figure 3.** Optimal steady state leaf area index ( $L_{opt}$ ) and  $g_1$  ( $g_{1,opt}$ ) compared with data from sites across Australia. The error bars show standard errors of measurements.

which suggested more severe water limitation (Figure 1b).  $Q_{PAR}$  increased  $L_{opt}$  when water was abundant but slightly decreased  $L_{opt}$  as water became limiting (Figure 1c; see equations (4) and (S3)).  $T_{max}$  reduced  $L_{opt}$  when water was abundant but slightly increased  $L_{opt}$  under water limitation (Figure 1d; see equation (S5)).

### 3.2. Site-Scale Evaluation of $L_{opt}$

Figure 2a shows  $L_{opt}$  for Australia and locations of site-scale LAI measurements.  $L_{opt}$  was predicted to decrease with increasing AI (Figure 2b). This response to water availability was consistent with both ground-based and satellite-derived (MODIS) estimates. Both predicted  $L_{opt}$  and MODIS were evaluated against ground-based measurements.  $L_{opt}$  had equivalent root-mean-square error (1.066 versus 1.170  $m^2 m^{-2}$ ) but more negative bias (mean of the difference between model and observations;  $-0.158$  versus 0.016  $m^2 m^{-2}$ ) than MODIS, suggesting that the model tended to underpredict in situ estimates, while MODIS was both higher and lower than ground data. Overall,  $L_{opt}$  values were of a similar accuracy to satellite estimates when compared to in situ measurements.  $L_{opt}$  correlated well with in situ LAI (Figure 2c;  $R^2 = 0.33$ ), suggesting that despite the difference

in scales between measurements and predictions, in situ LAI may not deviate much from the long-term equilibrium.  $L_{opt}$  predictions were also consistent with satellite-derived values (Figure 2d;  $R^2 = 0.6$ ).  $L_{opt}$  had a nonlinear relationship with both sets of measurements, showing that the model performance is close to measurements at low values of LAI but it tends to underpredict at high values of LAI. The model had comparable  $R^2$  values to statistical benchmark (GAM fits) of MODIS LAI for the sites (0.6 compared to 0.77; Table S2) but worse to that of the situ measurements and climate (0.33 compared to 0.68; Table S2). This better agreement with satellite-derived values than with in situ measurements is most likely to be due to a more consistent spatial sampling footprint between satellite and modeled data (0.06° or ~6 km).

Since the prediction of  $L_{opt}$  is balanced with  $g_1$  in the model, we also examined the optimal  $g_1$  ( $g_{1,opt}$ ) and in situ estimates to probe our results further (Figure 3; site details in Table S4). Measured LAI and  $g_1$  both declined with increasing AI. Predicted  $L_{opt}$  and  $g_{1,opt}$  tracked this decline in measured values. The model tended to overpredict LAI but systematically underpredict  $g_1$ .

### 3.3. Continental Evaluation

To evaluate model behavior at larger scales, we compared  $L_{opt}$  to satellite-derived estimates across Australian natural reserves (Figure 4a). Predicted  $L_{opt}$  captured the 9-year average from MODIS with an  $R^2$  of 0.7, a bias of  $-0.022$  ( $m^2 m^{-2}$ ), and a root-mean-square error of 0.370 ( $m^2 m^{-2}$ ). The model tended to slight overpredict LAI in most regions relative to the satellite-derived estimates and underpredict only at extreme wet coastal spots and at extreme dry center (Figure 4a). Again, the model had comparable  $R^2$  values to the statistical benchmark of MODIS LAI and climate (0.7 versus 0.81; Table S2). The nonlinear relationship in Figure 4b was consistent with the site-scale evaluation (Figure 2). Similar to the continental-wide pattern,  $L_{opt}$  was lower than MODIS at the extreme dry and wet sites in Northern Territory (Figure 4c). However, at the same MODIS LAI, the relative difference was smaller in the drier regions (higher AI; red versus blue dots in Figure 4d).

### 3.4. Change in $L_{opt}$ With Elevated $C_a$

To evaluate the modeled LAI response to the recent increase in  $C_a$  (340 to 389  $\mu\text{mol mol}^{-1}$ ), we compared the predictions against Donohue et al. (2013), who calculated the change of the slope of LAI against  $W_{MAP}$  in the driest areas ( $W_{MAP} < 400$   $\text{mm yr}^{-1}$ ) and found a 11.3% increase. We followed the same methodology and found the model predicted a 14.8% increase of slope. The predicted  $L_{opt}$  responses depended on water availability:  $L_{opt}$  remained relatively insensitive to  $C_a$  in wet areas, while it increased by up to 20% in dry areas (Figure 5a). We then used the model to predict the response to future changes (a doubling of  $C_a$  from 340 to 680  $\mu\text{mol mol}^{-1}$ ). The impact of future  $\text{CO}_2$  fertilization on model predictions was also determined by water availability: In the mesic regions (e.g.,  $W_{MAP} = 1,200$   $\text{mm}$ ;  $D = 0.5$   $\text{kPa}$ ), a doubling of  $C_a$  (340 to



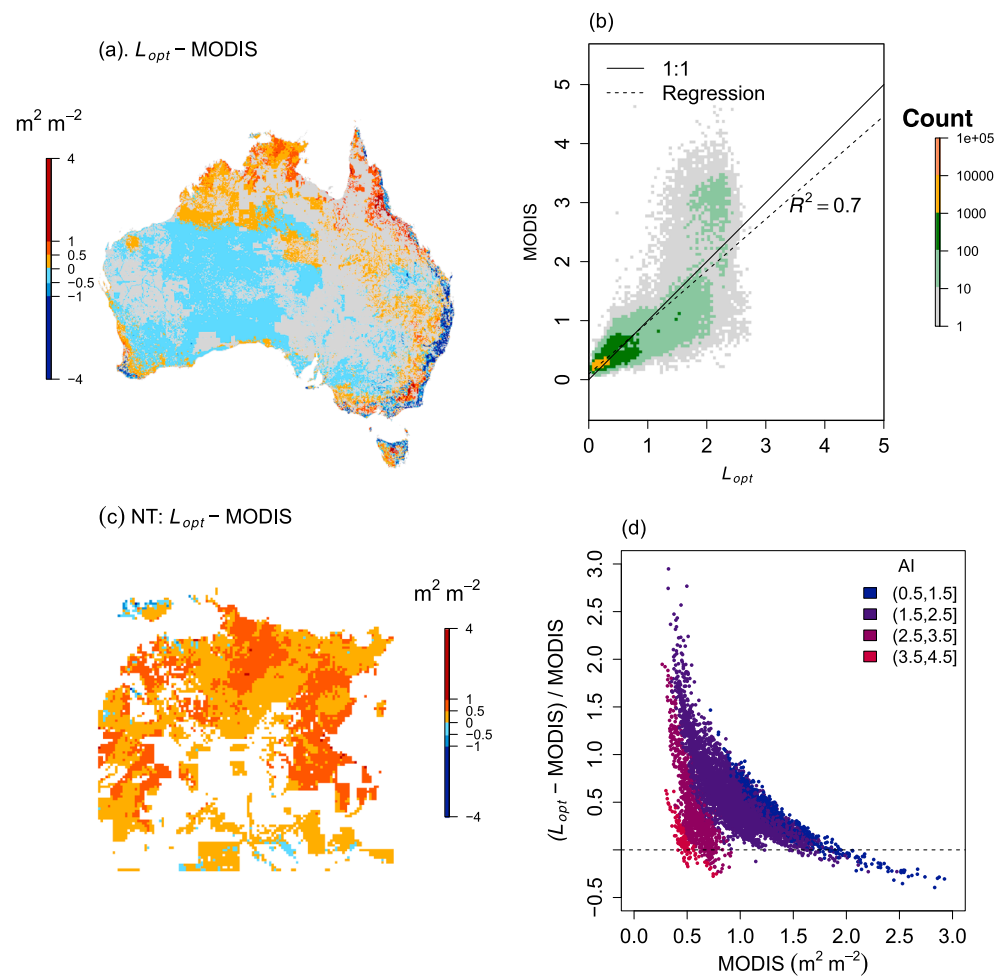


**Figure 4.**  $L_{opt}$  for Australian natural reserves compared to satellite products. (a)  $L_{opt}$  for natural reserves across Australia (gray indicates nonreserves). (b) Moderate Resolution Imaging Spectroradiometer (MODIS) versus  $L_{opt}$  with color-marked density. (c) The difference between  $L_{opt}$  and MODIS leaf area index (LAI) for Northern Territory (NT) natural reserves. (d) Relative difference between  $L_{opt}$  and MODIS LAI of NT, as function of MODIS LAI, with colors indicating aridity index.

$680 \mu\text{mol mol}^{-1}$ ) raised  $L_{opt}$  by  $\sim 20\%$  compared to a  $>100\%$  increase in xeric regions (e.g.,  $W_{MAP} = 400 \text{ mm}$ ;  $D = 3 \text{ kPa}$ ; Figure 5b).

We also examined how  $g_{1,opt}$  is predicted to change with increased  $C_a$  (340 to 389). On average,  $g_{1,opt}$  was predicted to be reduced by  $\sim 7.98\%$  (change of geometric mean) across Australia (Figure 5c), but the direction of change differed in dry versus wet areas. In dry areas, elevated  $C_a$  reduced  $g_{1,opt}$  (blue region in Figure 3c and orange lines in Figure 3d), while in wet areas,  $g_{1,opt}$  was predicted to increase ( $\sim 20\%$ ) increased with rising  $C_a$  (red region in Figure 3c and blue lines in Figure 3d). Since the predicted percentage increase of LAI and  $g_1$  to elevated  $C_a$  was nearly linear in both dry and wet conditions (Figures 5b and 5d, dashed lines), responses of LAI and  $g_1$  to rising  $C_a$  should follow the current trajectories at least to  $C_a \sim 680 \mu\text{mol mol}^{-1}$ .

## 4. Discussion

### 4.1. Model Performance

Predicting LAI is an important yet challenging step in the simulation of carbon and water fluxes, especially under climate change and rising  $C_a$ . We found that a parsimonious optimality model incorporating the concept of ecohydrological equilibrium could successfully predict long-term average LAI across the Australian

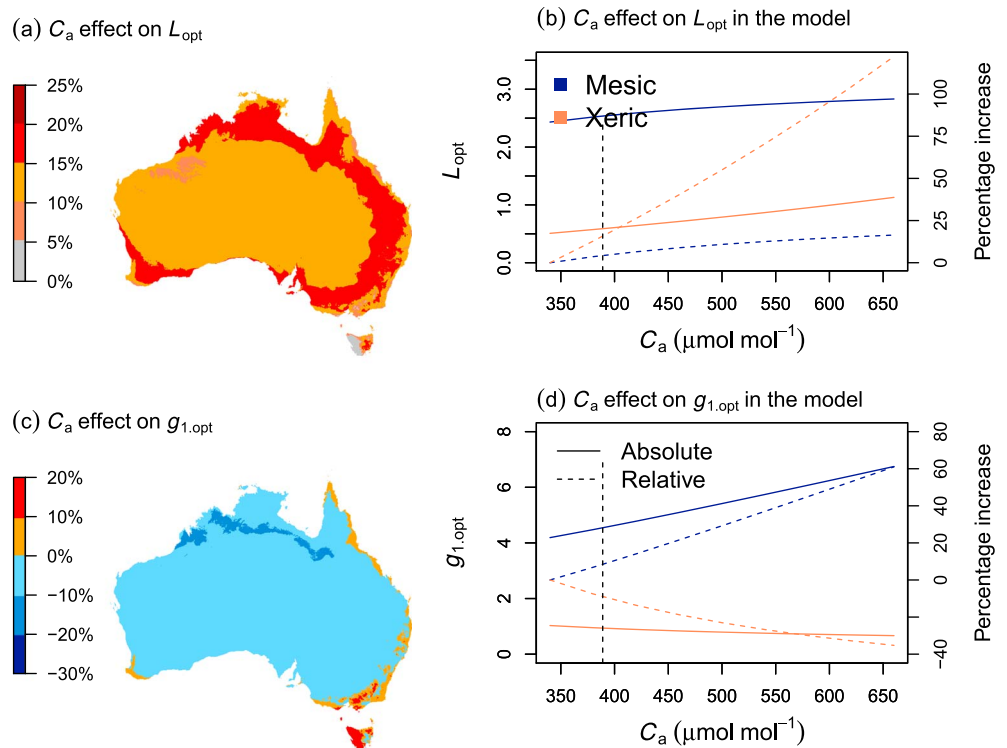


**Figure 5.** (a) Predicted effect of the 1980–2012 increase in  $C_a$  (from 340 to 389  $\mu\text{mol mol}^{-1}$ ) on  $L_{\text{opt}}$  in Australia. (b) Doubling  $C_a$  (340 to 680  $\mu\text{mol mol}^{-1}$ ) stimulates  $L_{\text{opt}}$  in the xeric regions by over 100% (orange dashed line) while  $\sim 20\%$  in mesic regions (blue dashed line). The dotted vertical lines mark 389  $\mu\text{mol mol}^{-1}$  corresponding to (a). (c) Predicted response of  $g_{1,\text{opt}}$  to the 1980–2012 increase in  $C_a$ . (d) Doubling  $C_a$  (340 to 680  $\mu\text{mol mol}^{-1}$ ) has different effects on  $g_1$  depending on water availability.

continent. This theory is thus a promising approach to incorporate into existing TBMs to improve predictions of foliage carbon allocation and LAI.

The optimality model showed good agreement with ground-based and satellite measurements. Previous assessments of satellite-derived products suggested an  $R^2$  of 0.56–0.85 among products (Fang et al., 2012, 2013; Hill et al., 2006; Garrigues et al., 2008). The model thus had an  $R^2$  comparable to that of satellite inter-product assessments. Our results suggested that LAI could be adequately predicted from consideration of the ecohydrological equilibrium. Since  $L_{\text{opt}}$  captured long-term mean MODIS, it should be possible to use  $L_{\text{opt}}$  in TBMs to reduce the current differences among models and satellite-derived products. The  $L_{\text{opt}}$  could, for example, be used as a target LAI for allocation routines, around which modeled LAI would vary dynamically according to phenology. Phenological variation of LAI could potentially be accounted for with a satellite-derived climatology (e.g., Broxton et al., 2014) or linked to existing process-based or optimization phenology models (e.g., Caldararu et al., 2014).

Although the model performed well overall, there was a discrepancy for high-LAI systems (Figure 4b). The predicted  $L_{\text{opt}}$  saturated at  $\sim 3 \text{ m}^2 \text{ m}^{-2}$ , while the observed values continued to increase. There are several potential causes for the discrepancy between our parsimonious model and observations at high LAI. First,  $R_m$ , which is assumed to be a constant, might be lower in higher-rainfall regions (Appendix A2). However, there is relatively little evidence to support such a variation in  $R_m$ , and the mechanism which would cause reduced  $R_m$  with higher water availability is not clear. In addition, nutrient limitation may be more important in regions with high LAI, and thus, consideration of nutrient availability may be necessary in these areas (McMurtrie & Dewar, 2013). Furthermore, the model does not take into account the decoupling between the vegetation and boundary layer, which may be significant in high-LAI systems (De Kauwe et al., 2017). These limitations of our simple, parsimonious approach could potentially be overcome if the theory were implemented in a TBM which treats these processes in more detail.

One key reason why our model improves LAI predictions is that it allows for variation in  $g_1$  (via  $g_s$ ) strategies in different climates. Lin et al. (2015) found, based on an analysis of a large database of leaf gas exchange measurements, that  $g_1$  varies with climate and plant functional type. Previous optimal LAI models either fixed stomatal behavior (Kergoat, 2002; Woodward & Lomas, 2004) or considered trade-offs between  $g_s$  and LAI (McMurtrie et al., 2008). Our approach optimized  $g_1$  simultaneously with LAI and thus represented a more realistic trade-off between the canopy (LAI) and leaf-level ( $g_1$ ) water use strategies. These predictions also potentially provide a means to inform TBM parameterization of  $g_1$ —currently using fixed parameters.

The pattern of  $g_{1,opt}$  agreed well with measurements, although there was a tendency to underpredict. There may be several reasons for this underprediction. First,  $g_{1,opt}$  is the ecosystem average  $g_1$  instead of only upper-canopy values. Consequently, one potential reason for overprediction of  $g_1$  at site scale is that measurements focus on the upper canopy.  $g_1$  varies with light availability and thus should be higher under light limitation (Campany et al., 2016). Another potential reason is the disagreement between  $g_1$  estimates on different scales: Plant water use efficiency (a function of  $g_1$ ; equation (S1)) measured on leaf and canopy scales were statistically different (Knauer et al., 2017; Medlyn et al., 2017). Moreover, the underprediction of  $g_1$  suggests that there may be potentially other trait-related costs (e.g., stem and root respiration and construction) that are currently unaccounted for in the model. The temporal distribution of rainfall may also add to the difference between observed and modeled  $g_1$  as stomatal conductance should respond not only to the amount of rainfall but also to the frequency (Lu et al., 2016).

An important benefit of this model is the ability to provide climate-constrained estimates of long-term changes in LAI with respect to increasing  $C_a$ . The increase of  $L_{opt}$  predicted by the model to rising  $C_a$  was consistent with satellite-derived observations. This evaluation focused on the effect of increased  $C_a$  alone; we assumed no change in long-term mean climate with rising  $C_a$ . The change of  $C_a$  during the evaluation period was accompanied by an average +7% of  $M_{MAP}$  (Donohue et al., 2009) and +8%  $D$  (Donohue et al., 2013). We did not consider these changes here because the impact of the  $M_{MAP}$  and  $D$  roughly canceled. However, in the future, rising  $C_a$  could be accompanied by larger changes in  $M_{MAP}$ . The sensitivity of  $L_{opt}$  to water availability in Australia suggests that the uncertainty in climate predictions of rainfall for Australia (e.g.,  $\pm 100\%$  with large intermodel variations; Mehran et al., 2014) could very likely transfer into uncertain vegetation feedbacks through changes in LAI.

The model also provides insights into the trade-off between LAI and  $g_1$  in the context of rising  $C_a$ . Previous studies of stomatal behavior (Manzoni et al., 2013; Lu et al., 2016; Wolf et al., 2016; Prentice et al., 2014) have examined leaf-scale optimization but generally do not consider whole-plant trade-offs such as the balance between stomatal conductance and LAI (but see Kelly et al., 2015). Leaf-scale optimization models generally predict no change in  $g_1$  under elevated  $C_a$ . As a result, larger scale studies have also assumed constant  $g_1$  with increasing  $C_a$  when assessing LAI responses (e.g., Cheng et al., 2017; Donohue et al., 2017; Yang et al., 2016). Here the predicted  $g_{1,opt}$  had distinct responses to rising  $C_a$  under different water availability scenarios. Under dry conditions, the model predicted reduced  $g_{1,opt}$  and increased  $L_{opt}$  with elevated  $C_a$ , suggesting that it is beneficial for the plant to use the increased available C to grow leaves. Increased LAI in water-limited areas brings a double benefit to the plant because it increases both the transpiration fraction (equation (1)) and PAR interception (equations (S8a) and (S8b)). Reduced  $g_1$  also indicates a decrease in the marginal carbon cost of water (Cowan & Farquhar, 1977), which suggests that elevated  $C_a$  releases water stress to some extent. Under wetter conditions, both  $g_{1,opt}$  and  $L_{opt}$  and predicted to increase slowly with rising  $C_a$ , indicating the diminishing return from increasing  $C_a$  with increasing water availability. Both the direction and the magnitude of  $g_1$  responses to  $C_a$  under different water availability are consistent with the findings in Schymanski et al. (2015), who predicted that marginal carbon cost of water would reduce by  $\sim 14\%$  in a dry site but increase  $\sim 13\%$  in a wet site with 20% increase of  $C_a$ . The predicted change in  $g_{1,opt}$  with  $C_a$  adds to our general understanding of marginal carbon cost of water use: Previous meta-analyses of elevated  $C_a$  experiments not only found overall no change in  $g_1$  with increasing  $C_a$  (e.g., Ainsworth & Rogers, 2007; Medlyn et al., 2001; but see Keenan et al., 2013) but also indicated variation across experiments. Our model specifically predicts that  $g_1$  would increase with increased  $C_a$  in wet conditions and decrease in dry conditions—a testable hypothesis.

#### 4.2. Alternative Model Assumptions

Our optimality model included two important empirical assumptions: (1) Plant transpiration is constrained to be a function of mean annual precipitation and LAI (equations (1) and (2)), and (2) maintenance respiration,

leaf mass per area, and life lifespan do not vary with climate. We tested alternative assumptions in each of these two areas, but none led to better model performance (Appendix A). The model prioritized parsimony and did not incorporate assumptions that did not improve model performance. However, these parameters are inputs to the model and can thus be changed upon the emergence of new theories and evidence.

Water availability to the plant, or transpiration in the model, is crucial to model predictions. The model showed that  $L_{\text{opt}}$  was sensitive to water input and thus the uncertainty in water availability contributed to the errors in the predictions. Water resources such as groundwater and surface flow are not included in the model but can be used for transpiration in certain regions (Evaristo et al., 2015; Liu et al., 2017). Topography has impacts on local water availability and thus plant water use strategies (Méndez-Toribio et al., 2017). Incorporation of the ecohydrological equilibrium theory into a more detailed TBM which accounts for topography and soil type would allow these effects to be incorporated in LAI predictions.

The temporal variation of water availability is also important to determine equilibrium LAI. In extreme cases such as tropical savanna in the Northern Territory, the majority of rainfall falls during the wet half of the year (Cernusak et al., 2011). The equilibrium LAI for average rainfall in dry and wet seasons would be very different. Indeed, the model agreed more with the long-term average MODIS LAI estimates than ground-based LAI, which are typically one-off measurements (Figure 2), suggesting the potential importance of variability of water availability and other parameters (e.g., respiration). Here we used an annual time step for simplicity. However, in strongly seasonal rainfall environments, it may be more appropriate to evaluate  $L_{\text{opt}}$  on subannual time scales. Hence, we aim to predict optimal seasonality along with  $L_{\text{opt}}$  in future developments of the model.

Empirical studies have suggested variation in the four plant traits used in the model ( $R_m$ ,  $J_{\text{max}}$ ,  $M_{\text{arear}}$ , and  $t_f$ ) with climate (Ali et al., 2015; Atkin et al., 2015; Dong et al., 2017; Heskell et al., 2016; Wright et al., 2004). This variation is potentially important to modeling carbon and water (Pappas et al., 2016). We examined existing data sets for these relationships but only found weak correlations, which, when implemented into the model, did not improve model performance nor substantially modify model behavior (Appendix A). We also did not discover any relationship between our literature-compiled values of  $J_{\text{max}}$  across Australia and climate (Figure S1). Consequently, we assumed here that  $R_m$ ,  $J_{\text{max}}$ ,  $M_{\text{arear}}$ , and  $t_f$  were independent of climate. However, including empirical relationships between these parameters and  $W_{\text{MAP}}$  tends to increase predicted LAI where high LAI is observed (Figures A2 and A3). As a result, including variable parameters may help reduce the discrepancy between the modeled and observed LAI at high LAI (Figure 4d). New data sets and theories for variation in traits with climate are emerging: The correlation between plant traits and climate could be explained by physiological trade-offs (Onoda et al., 2017) and thus should be predictable by optimality models (e.g., Xu et al., 2017). The model is flexible enough to incorporate these new theories.

There is substantial evidence that leaf photosynthesis and respiration rates depend on leaf nitrogen content (Norby et al., 2017; Ryan, 1991). Nitrogen and phosphorus limitation have been suggested to be particularly common in Australian ecosystems due to the old, weathered soils (Chapin et al., 1986; Elser et al., 2007; Ellsworth et al., 2017; Wild, 1958). The lack of representation of nutrient limitation may contribute to the underprediction at high LAI seen in Figure 4d. McMurtrie et al. (2008) included a dependence of photosynthetic rate on leaf nitrogen content and considered the three-way trade-off between leaf nitrogen, stomatal conductance, and LAI. However, their approach requires knowledge of the canopy nitrogen uptake rate, which precludes application at the continental scale. To determine whether omitting nutrient availability impacts model success, we fitted GAMs to observed LAI and climate, with and without soil nitrogen and phosphorus as predictor variables. We found that including soil nutrients in the GAM did not capture more variation of measured LAI (Table S2). We also found that the water and carbon constrained  $L_{\text{opt}}$  agreed with existing data well, despite not incorporating the impacts of nutrient limitation. However, this result does not invalidate the importance of nutrient limitation, due to correlations between soil nutrient availability and water availability (Table S3). The impacts of nutrient limitations may thus already be incorporated in the water limitation.

$J_{\text{max}}$  and  $R_m$  are known to be sensitive to temperature in the short term, but here we ignored this temperature dependence because both  $J_{\text{max}}$  and  $R_m$  have been reported to acclimate to growth temperature (Aspinwall et al., 2016; Reich et al., 2016; Smith et al., 2015). We found no correlation between  $J_{\text{max}}$  and  $R_m$  with temperature (section A2, Figure S1). As a result, we decided to use constant values of  $J_{\text{max}}$  and  $R_m$ . Temperature

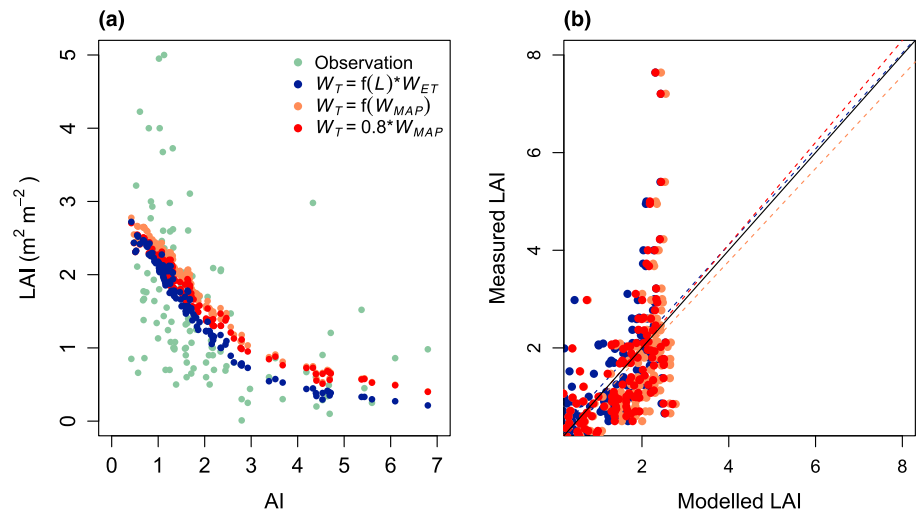


**Figure A1.** Impact of different transpiration fraction assumptions on  $L_{opt}$ . (a) The impact of different assumptions along the aridity index (gradient) and how they compared to observations. The  $L_{opt}$  from final model are the blue dots. “ $W_T = f(W_{MAP})$ ” means substituting equation (1) with a constant fraction of 1. “ $W_T = 0.8 * W_{MAP}$ ” means neither equation (1) nor (2) is used but instead a constant fraction is implemented (0.8). (b) Scatterplot of measured and modeled leaf area index with the solid line being 1:1 ratio and dashed line regression colored by assumptions.

dependence could be explored further in future; the model is flexible and could adopt a temperature dependence if necessary.

## 5. Conclusion

We showed that a parsimonious optimization model incorporating ecohydrological theory can accurately predict long-term average LAI in Australian ecosystems. The inputs (i.e., climate) and outputs (i.e., LAI and  $g_1$ ) of the model are all being measured and thus enable convenient application and evaluation. Although set to be constant or calculated via empirical equations, all the parameters used in the model can be taken as inputs enabling accommodation to different purposes of studies. This approach could readily be incorporated into vegetation models to set a target long-term LAI, with the short-term variation modified as a function of water balance dynamics and phenology. Although the evaluation is limited to Australia, these findings may also apply to other water-limited ecosystems. Consequently, we suggest that TBMs could constrain leaf area predictions under climate change and rising  $C_a$  in water-limited regions to realistic values by incorporating a climate-constrained trade-off between leaf area and canopy conductance into their foliage submodel.

## Appendix A: Alternative Assumptions

There are several potential options to calculate the key parameters (i.e.,  $M_{area}$ ,  $t_f$ ,  $W_T$ , and  $R_m$ ) in the model. It is therefore important to investigate how the underlying assumptions differ among equations and how those differences affect the predictions. In the following section, we compared the alternative functions to those implemented, illustrated the differences among the assumptions, and explained the reasoning behind our choice of assumptions for the final model.

### A1. The Transpiration Fraction

The final model included the assumptions that the transpiration fraction varies with LAI (equation (1); Wang et al., 2014) and with precipitation (equations (2); Zhang et al., 2001). An alternative potential assumption is to take transpiration as a constant fraction (0.8) of precipitation as in McMurtrie et al. (2008). A constant transpiration fraction resulted in higher prediction at low observed LAI (red dots and lines in Figures A1a and A1b). Including the Zhang et al. (2001) relationship with precipitation only slightly improved the result (orange dots and lines in Figures A1a and A1b). Assuming the transpiration fraction to be a function of LAI gave the lowest results of all three assumptions tested here (blue dots and lines in Figures A1a and A1b).

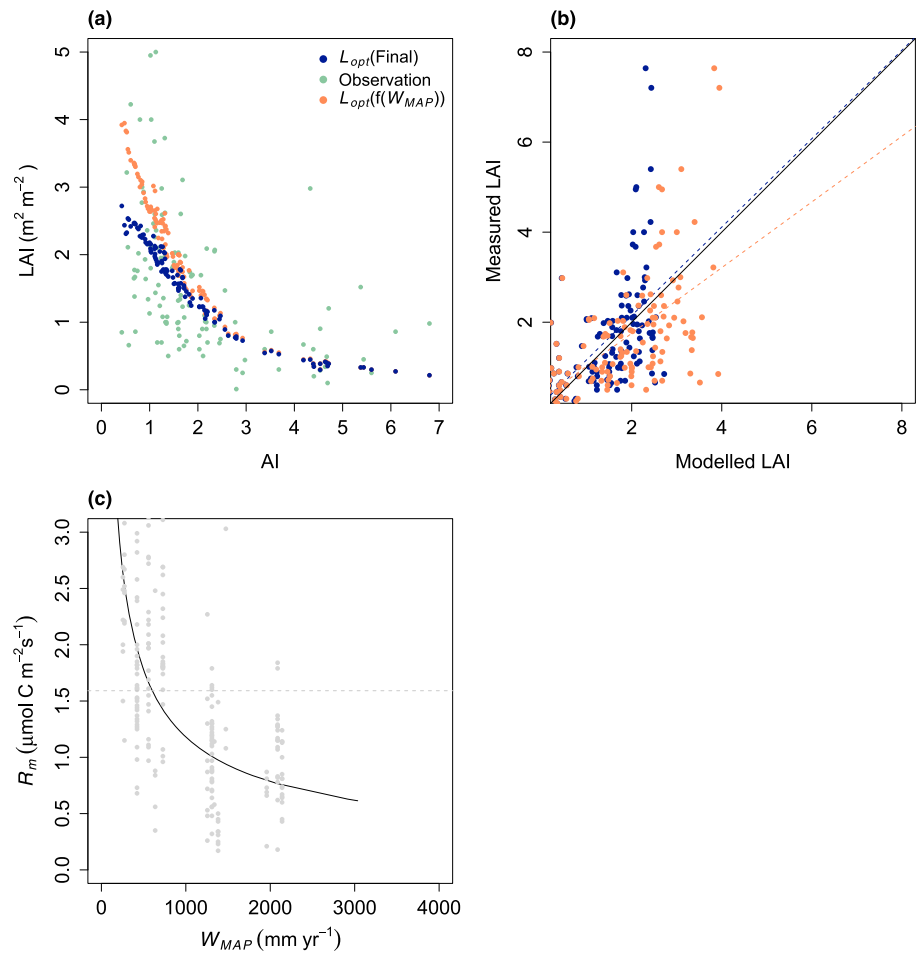


**Figure A2.** Comparison of the impacts of different  $R_m$  assumptions. (a)  $L_{opt}$  under different  $R_m$  assumptions compared to the in situ measurements along an aridity index gradient. Note that the final model uses constant  $R_m$  (blue dots). (b) The difference between constant  $R_m$  and the final model. (c) The tested  $R_m$ - $W_{MAP}$  relationship with the dashed line indicating the value used in the final model and gray dots being the measurements from the Australian subset of the GLOBRESP data set (Atkin et al., 2015). Note that different assumptions are used here and in Figure A3d.

Although calculating transpiration fraction as a function of LAI added complexity and required iteration, we included this assumption in the final model for its fitness to data (blue line in Figure A1b). Alternatively, it may be viable to reduce prediction error at high AI by increasing respiration cost at high AI empirically (see the following section).

## A2. Maintenance Respiration

$R_m$ , maintenance respiration per unit leaf area ( $\mu\text{mol m}^{-2} \text{ leaf s}^{-1}$ ), is a key factor in determining the cost of leaf growth. The final model assumed a constant value ( $1.59 \mu\text{mol m}^{-2} \text{ s}^{-1}$ ). This section explained the alternative assumptions we considered for  $R_m$  and showed how they affected the model predictions. We fitted an empirical relationship between  $R_m$  and  $W_{MAP}$  ( $R^2 = 0.36$ ) to data from the Australian subset of the GLOBRESP data set (Atkin et al., 2015):

$$\ln(R_m) = a_r \cdot \ln(W_{MAP}) + b_r \quad (\text{A1})$$

where  $a_r$  and  $b_r$  are fitted parameters,  $-0.589$  and  $4.235$ , respectively.

A constant  $R_m$  was chosen over the empirical relationship for the final model because: (i) The  $R_m$ - $W_{MAP}$  relationship does not improve prediction at low in situ LAI (AI from 3 to 7 in Figure A2a); (ii) the final

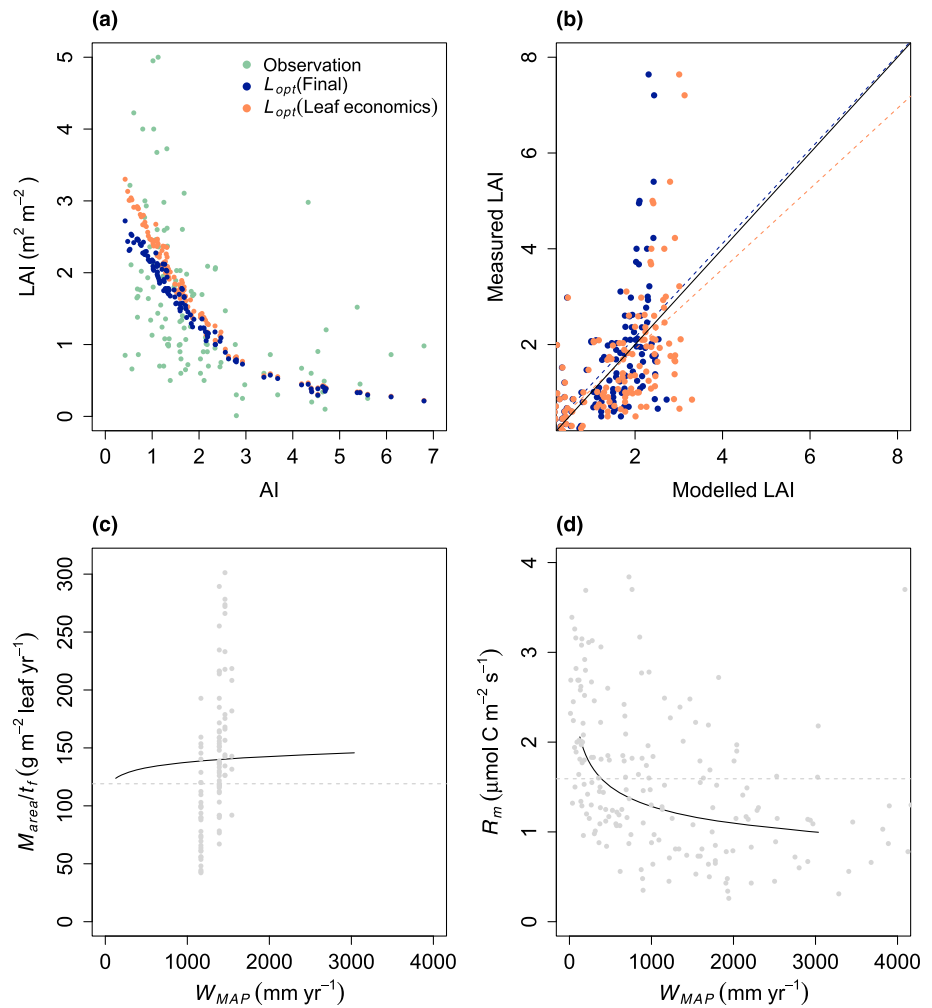


**Figure A3.**  $L_{opt}$  based on leaf economics compared to that of the final model. (a)  $L_{opt}$  based on leaf economics and final model compared to the measurements along an aridity index gradient. (b) The scatterplots of measurements against leaf economics and final model. (c) The change of leaf carbon investment ( $M_{area}/t_f$ ) over a rainfall gradient. (d) The change of  $R_m$  based on  $M_{area}$  over a rainfall gradient. The solid lines show the regression. The gray dashed lines in (c) and (d) mark the values used in the final model. The gray dots are measurements.

model captured the observations better overall (blue dashed line was closer to 1:1 ratio than the orange dashed line in Figure A2b); and (iii) a climate-modified  $R_m$  added unnecessary complexity to the model assumptions.

Equation (A1) predicts an exponential decline of  $R_m$  with  $W_{MAP}$  (Figure A2c). However, the impact of incorporating this relationship on model predictions did not follow the same pattern. The difference between the two assumptions was negligible at low LAI because when LAI is very low,  $R_m$  has limited impact on the optimization compared to the exponential relationships of  $f_{APAR}$  (equation (S8a)) and transpiration fraction to LAI (equation (1)). However, at high LAI, both  $f_{APAR}$  and transpiration fraction were nearly saturated and thus a small change in  $R_m$  has a large impact on the prediction.

The impact of the  $R_m$  assumption would be larger if the model did not include the transpiration fraction to LAI relationship. As mentioned in the previous section, the model prediction could be improved by either incorporating the transpiration fraction-LAI relationship or a climate-modified  $R_m$ . The transpiration fraction-LAI assumption is more empirically justifiable but requires iteration to solve. It may thus be possible to improve the computational efficiency of the model by using an empirical  $R_m$ - $W_{MAP}$  relationship instead of the transpiration fraction-LAI relationship, but this risks the limited applicability of the empirical relationship.

### A3. Leaf Economics

The parameters describing leaf economics in the model are  $R_m$ ,  $M_{\text{area}}$  and  $t_f$  which are assumed constant in this study (section 2 and Table S1). Previous studies (e.g., Wright et al., 2004) have suggested correlations among  $R_m$ ,  $M_{\text{area}}$  and  $t_f$ . In this section, we test the alternatives of calculating  $R_m$ ,  $M_{\text{area}}$  and  $t_f$  with empirical relationships and the impacts on predictions.

$t_f$  correlates best with  $M_{\text{area}}$  according to GLOPNET data set ( $R^2 = 0.44$ ; Wright et al., 2004):

$$\ln(t_f) = a_f \cdot \ln(M_{\text{area}}) - b_f \quad (\text{A2})$$

where  $a_f$  and  $b_f$  are fitted parameters equal to 1.14 and  $-5.64$ , respectively. Similarly,  $R_m$  can be expressed as a function of  $M_{\text{area}}$ :

$$\ln(R_m) = a_{rm} \cdot \ln(M_{\text{area}}) - b_{rm} \quad (\text{A3})$$

where  $a_{rm}$  and  $b_{rm}$  are fitted parameters and equal to 0.63 and  $-2.94$ , respectively. Here equation (A3) was derived from the Australian subset of GLOBRESP (Atkin et al., 2015) with an  $R^2$  of 0.25.  $M_{\text{area}}$  correlates best with mean annual precipitation according to the same data set ( $R^2 = 0.22$ ; Atkin et al., 2015):

$$\ln(M_{\text{area}}) = a_m \cdot \ln(W_{\text{MAP}}) + b_m \quad (\text{A4})$$

where  $a_m$  and  $b_m$  are fitted parameters with values of  $-0.36$  and  $7.52$ , respectively.

Although these relationships are statistically significant, we did not implement them in the final model because making  $M_{\text{area}}$  and  $t_f$  functions of climate had no effect on model predictions in dry regions ( $AI > 2$  in Figures A3a and A3b). The reason is that the carbon investment per unit time (proportional to  $M_{\text{area}}/t_f$ ) and  $R_m$  is relatively insensitive to climate (Figures A3c and A3d). (ii) The regression line between the final model and observations was closer to 1:1 ratio than the one based on leaf economics (blue versus orange dashed lines in Figure A3b). For parsimony, the final model thus used the constant  $M_{\text{area}}$  and  $t_f$ . The values  $M_{\text{area}}$  and  $t_f$  in the final model were based on GLOPNET, while the  $M_{\text{area}}$  correlation with  $W_{\text{MAP}}$  was derived from GLOBRESP. The reason we tested the correlation from GLOBRESP is that the same correlation is not significant in GLOPNET. We chose to use the constant values of  $M_{\text{area}}$  and  $t_f$  from GLOPNET because  $t_f$  is not reported in GLOBRESP. We thus used values from one data set for consistency. Consequently, the gray line in Figure A3c was not the mean of the dots.

#### Acknowledgments

J.Y. was supported by a PhD scholarship from the Hawkesbury Institute for the Environment, Western Sydney University. Martin De Kauwe acknowledges support from the ARC Centre of Excellence for Climate Extremes (CE170100023). This research was undertaken with the assistance of resources from the National Computational Infrastructure (NCI), which is supported by the Australian Government. The model is constructed in R, and the code is fully open via the link [https://bitbucket.org/Jinyan\\_Jim\\_Yang/lai-model-perm-19jan2018/](https://bitbucket.org/Jinyan_Jim_Yang/lai-model-perm-19jan2018/) overview. NCI website provides the climate data (<http://dapds00.nci.org.au/thredds/catalog.html>) and MODIS LAI (<http://remote-sensing.nci.org.au/u39/public/html/index.shtml>). Some of the ground-based LAI data were obtained through TERN AusCover (<http://www.auscover.org.au>). TERN is Australia's land-based ecosystem observatory delivering data streams to enable environmental research and management (TERN, <http://www.tern.org.au>). TERN is a part of Australia's National Collaborative Research Infrastructure Strategy (NCRIS, <https://www.education.gov.au/national-collaborative-research-infrastructure-strategy-ncris>).

#### References

- Abramowitz, G. (2005). Towards a benchmark for land surface models. *Geophysical Research Letters*, 32, L22702. <https://doi.org/10.1029/2005GL024419>
- Ainsworth, E. A., & Rogers, A. (2007). The response of photosynthesis and stomatal conductance to rising [CO<sub>2</sub>]: Mechanisms and environmental interactions. *Plant, Cell & Environment*, 30(3), 258–270. <https://doi.org/10.1111/j.1365-3040.2007.01641.x>
- Ali, A. A., Xu, C., Rogers, A., McDowell, N. G., Medlyn, B. E., Fisher, R. A., et al. (2015). Global-scale environmental control of plant photosynthetic capacity. *Ecological Applications*, 25(8), 2349–2365. <https://doi.org/10.1890/14-2111.1>
- Anav, A., Friedlingstein, P., Kidston, M., Bopp, L., Ciais, P., Cox, P., et al. (2013). Evaluating the land and ocean components of the global carbon cycle in the CMIP5 Earth system models. *Journal of Climate*, 26(18), 6801–6843. <https://doi.org/10.1175/JCLI-D-12-00417.1>
- Aspinwall, M. J., Drake, J. E., Company, C., Vårhammar, A., Ghannoum, O., Tissue, D. T., et al. (2016). Convergent acclimation of leaf photosynthesis and respiration to prevailing ambient temperatures under current and warmer climates in *Eucalyptus tereticornis*. *The New Phytologist*, 212(2), 354–367. <https://doi.org/10.1111/nph.14035>
- Atkin, O. K., Bloomfield, K. J., Reich, P. B., Tjoelker, M. G., Asner, G. P., Bonal, D., et al. (2015). Global variability in leaf respiration in relation to climate, plant functional types and leaf traits. *The New Phytologist*, 206(2), 614–636. <https://doi.org/10.1111/nph.13253>
- Ball, J. T., Woodrow, I. E., & Berry, J. A. (1987). A model predicting stomatal conductance and its contribution to the control of photosynthesis under different environmental conditions. *Progress in Photosynthesis Research*, 221–224. [https://doi.org/10.1007/978-94-017-0519-6\\_48](https://doi.org/10.1007/978-94-017-0519-6_48)
- Beerling, D., & Woodward, F. (2001). *Vegetation and the terrestrial carbon cycle modelling the first 400 million years*. Cambridge: Cambridge University Press. <https://doi.org/10.1017/CBO9780511541940>
- Beringer, J., & McHugh, I. (2015a). Leaf area index data, Victorian Dry Eucalypt SuperSite, Whroo, 2014. TERN Australian SuperSite Network. <http://www.supersites.net.au/knb/metacat/supersite.295.5/html>. Accessed on 1/11/2017.
- Beringer, J., & McHugh, I. (2015b). Leaf area index data, Victorian Dry Eucalypt SuperSite, Whroo, 2015. TERN Australian SuperSite Network. <http://www.supersites.net.au/knb/metacat/supersite.292.6/html>. Accessed on 1/11/2017.
- Bernacchi, C. J., Singaas, E. L., Pimentel, C., Portis, A. R., & Long, S. P. (2001). Improved temperature response functions for models of Rubisco-limited photosynthesis. *Plant, Cell and Environment*, 24(2), 253–259. <https://doi.org/10.1046/j.1365-3040.2001.00668.x>
- Bradford, M. (2015). Leaf area index data, FNQ Rainforest SuperSite, Robson Creek, Core 1 ha, 2014. TERN Australian SuperSite Network. <http://www.supersites.net.au/knb/metacat/supersite.150.7/html>. Accessed on 1/11/2017.



- Broxton, P. D., Zeng, X., Sulla-Menashe, D., & Troch, P. A. (2014). A global land cover climatology using MODIS data. *Journal of Applied Meteorology and Climatology*, 53(6), 1593–1605. <https://doi.org/10.1175/JAMC-D-13-0270.1>
- Caldararu, S., Purves, D. W., & Palmer, P. I. (2014). Phenology as a strategy for carbon optimality: A global model. *Biogeosciences*, 11(3), 763–778. <https://doi.org/10.5194/bg-11-763-2014>
- Campany, C. E., Tjoelker, M. G., von Caemmerer, S., & Duursma, R. A. (2016). Coupled response of stomatal and mesophyll conductance to light enhances photosynthesis of shade leaves under sunflecks. *Plant, Cell & Environment*, 39(12), 2762–2773. <https://doi.org/10.1111/pce.12841>
- Cernusak, L. A., Hutley, L. B., Beringer, J., Holtum, J. A. M., & Turner, B. L. (2011). Photosynthetic physiology of eucalypts along a sub-continental rainfall gradient in northern Australia. *Agricultural and Forest Meteorology*, 151(11), 1462–1470. <https://doi.org/10.1016/j.agrformet.2011.01.006>
- Chapin, F., Vitousek, P., & Cleve, K. (1986). The nature of nutrient limitation in plant communities. *The American Naturalist*, 127(1), 48–58.
- Cheng, L., Zhang, L., Wang, Y.-P., Canadell, J. G., Chiew, F. H. S., Beringer, J., et al. (2017). Recent increases in terrestrial carbon uptake at little cost to the water cycle. *Nature Communications*, 8(1), 110. <https://doi.org/10.1038/s41467-017-00114-5>
- Cowan, I. R., & Farquhar, G. D. (1977). Stomatal function in relation to leaf metabolism and environment. *Symposia of the Society for Experimental Biology*, 31(1973), 471–505.
- De Kauwe, M. G., Lin, Y., Wright, I. J., Medlyn, B. E., Crous, K. Y., Ellsworth, D. S., et al. (2016). A test of the 'one-point method' for estimating maximum carboxylation capacity from field-measured, light-saturated photosynthesis. *The New Phytologist*, 210(3), 1130–1144. <https://doi.org/10.1111/nph.13815>
- De Kauwe, M. G., Medlyn, B. E., Knauer, J., & Williams, C. A. (2017). Ideas and perspectives: How coupled is the vegetation to the boundary layer? *Biogeosciences*, 14(19), 4435–4453. <https://doi.org/10.5194/bg-14-4435-2017>
- De Kauwe, M. G., Medlyn, B. E., Zaehle, S., Walker, A. P., Dietze, M. C., Wang, Y. P., et al. (2014). Where does the carbon go? A model-data intercomparison of vegetation carbon allocation and turnover processes at two temperate forest free-air CO<sub>2</sub> enrichment sites. *The New Phytologist*, 203(3), 883–899. <https://doi.org/10.1111/nph.12847>
- Dong, N., Prentice, I. C., Evans, B. J., Caddy-Retalic, S., Lowe, A. J., & Wright, I. J. (2017). Leaf nitrogen from first principles: Field evidence for adaptive variation with climate. *Biogeosciences*, 14(2), 481–495. <https://doi.org/10.5194/bg-14-481-2017>
- Donohue, R. J., McVicar, T. R., & Roderick, M. L. (2009). Climate-related trends in Australian vegetation cover as inferred from satellite observations, 1981–2006. *Global Change Biology*, 15(4), 1025–1039. <https://doi.org/10.1111/j.1365-2486.2008.01746.x>
- Donohue, R. J., Roderick, M. L., McVicar, T. R., & Farquhar, G. D. (2013). Impact of CO<sub>2</sub> fertilization on maximum foliage cover across the globe's warm, arid environments. *Geophysical Research Letters*, 40, 3031–3035. <https://doi.org/10.1002/grl.50563>
- Donohue, R. J., Roderick, M. L., McVicar, T. R., & Yang, Y. (2017). A simple hypothesis of how leaf and canopy-level transpiration and assimilation respond to elevated CO<sub>2</sub> reveals distinct response patterns between disturbed and undisturbed vegetation. *Journal of Geophysical Research: Biogeosciences*, 122, 168–184. <https://doi.org/10.1002/2016JG003505>
- Duursma, R. A. (2015). Plantecophys—An R package for analysing and modelling leaf gas exchange data. *PLoS One*, 10(11), 1–13. <https://doi.org/10.1371/journal.pone.0143346>
- Duursma, R. A., Gimeno, T. E., Boer, M. M., Crous, K. Y., Tjoelker, M. G., & Ellsworth, D. S. (2016). Canopy leaf area of a mature evergreen eucalyptus woodland does not respond to elevated atmospheric [CO<sub>2</sub>] but tracks water availability. *Global Change Biology*, 22(4), 1666–1676. <https://doi.org/10.1111/gcb.13151>
- Eagleson, P. S. (1982). Ecological optimality in water-limited natural soil vegetation systems: 1. Theory and hypothesis. *Water Resources Research*, 18(2), 325–340. <https://doi.org/10.1029/WR018i002p00325>
- Eamus, D., & Cleverly, J. (2015a). Leaf area index data, Alice Mulga SuperSite, 2014. TERN Australian SuperSite Network. <http://www.supersites.net.au/knb/metacat/supersite.375.4/html>. Accessed on 1/11/2017.
- Eamus, D., & Cleverly, J. (2015b). Leaf area index data, Alice Mulga SuperSite, 2015. TERN Australian SuperSite Network. <http://www.supersites.net.au/knb/metacat/supersite.377.4/html>. Accessed on 1/11/2017.
- Ellis, T. W., & Hatton, T. J. (2008). Relating leaf area index of natural eucalypt vegetation to climate variables in southern Australia. *Agricultural Water Management*, 95(6), 743–747. <https://doi.org/10.1016/j.agwat.2008.02.007>
- Ellsworth, D. S., Anderson, I. C., Crous, K. Y., Cooke, J., Drake, J. E., Gherlenda, A. N., et al. (2017). Elevated CO<sub>2</sub> does not increase eucalypt forest productivity on a low-phosphorus soil. *Nature Climate Change*, 7(4), 279–282. <https://doi.org/10.1038/nclimate3235>
- Elser, J. J., Bracken, M. E. S., Cleland, E. E., Gruner, D. S., Harpole, W. S., Hillebrand, H., et al. (2007). Global analysis of nitrogen and phosphorus limitation of primary producers in freshwater, marine and terrestrial ecosystems. *Ecology Letters*, 10(12), 1135–1142. <https://doi.org/10.1111/j.1461-0248.2007.01113.x>
- Evaristo, J., Jasechko, S., & McDonnell, J. J. (2015). Global separation of plant transpiration from groundwater and streamflow. *Nature*, 525(7567), 91–94. <https://doi.org/10.1038/nature14983>
- Fang, H., Jiang, C., Li, W., Wei, S., Baret, F., Chen, J. M., et al. (2013). Characterization and intercomparison of global moderate resolution leaf area index (LAI) products: Analysis of climatologies and theoretical uncertainties. *Journal of Geophysical Research: Biogeosciences*, 118, 529–548. <https://doi.org/10.1002/jgrg.20051>
- Fang, H., Wei, S., & Liang, S. (2012). Validation of MODIS and CYCLOPES LAI products using global field measurement data. *Remote Sensing of Environment*, 119, 43–54. <https://doi.org/10.1016/j.rse.2011.12.006>
- Garrigues, S., Lacaze, R., Baret, F., Morisette, J. T., Weiss, M., Nickeson, J. E., et al. (2008). Validation and intercomparison of global leaf area index products derived from remote sensing data. *Journal of Geophysical Research*, 113, G02028. <https://doi.org/10.1029/2007JG000635>
- Gimeno, T. E., Crous, K. Y., Cooke, J., O'Grady, A. P., Ósváldsson, A., Medlyn, B. E., & Ellsworth, D. S. (2016). Conserved stomatal behaviour under elevated CO<sub>2</sub> and varying water availability in a mature woodland, edited by D. Whitehead. *Functional Ecology*, 30(5), 700–709. <https://doi.org/10.1111/1365-2435.12532>
- Heskel, M. A., O'Sullivan, D. S., Reich, P. B., Tjoelker, M. G., Weerasinghe, L. K., Penillard, A., et al. (2016). Convergence in the temperature response of leaf respiration across biomes and plant functional types. *Proceedings of the National Academy of Sciences*, 113(14), 3832–3837. <https://doi.org/10.1073/pnas.1520282113>
- Hill, M. J., Senarath, U., Lee, A., Zeppel, M., Nightingale, J. M., Williams, R. J., & McVicar, T. R. (2006). Assessment of the MODIS LAI product for Australian ecosystems. *Remote Sensing of Environment*, 101(4), 495–518. <https://doi.org/10.1016/j.rse.2006.01.010>
- Iio, A., Hikosaka, K., Anten, N. P. R., Nakagawa, Y., & Ito, A. (2014). Global dependence of field-observed leaf area index in woody species on climate: A systematic review. *Global Ecology and Biogeography*, 23(3), 274–285. <https://doi.org/10.1111/geb.12133>
- Jin, Y., & Goulden, M. L. (2014). Ecological consequences of variation in precipitation: Separating short- versus long-term effects using satellite data. *Global Ecology and Biogeography*, 23(3), 358–370. <https://doi.org/10.1111/geb.12135>

- Keenan, T. F., Hollinger, D. Y., Bohrer, G., Dragoni, D., Munger, J. W., Schmid, H. P., & Richardson, A. D. (2013). Increase in forest water-use efficiency as atmospheric carbon dioxide concentrations rise. *Nature*, *499*(7458), 324–327. <https://doi.org/10.1038/nature12291>
- Kelly, J. W. G. (2013). Productivity and water use of Australian tree species under climate change, PhD Thesis, Macquarie University.
- Kelly, J. W. G., Duursma, R. A., Atwell, B. J., Tissue, D. T., & Medlyn, B. E. (2015). Drought × CO<sub>2</sub> interactions in trees: A test of the low-intercellular CO<sub>2</sub> concentration (C<sub>i</sub>) mechanism. *The New Phytologist*, *209*(4), 1600–1612. <https://doi.org/10.1111/nph.13715>
- Kergoat, L. (1998). A model for hydrological equilibrium of leaf area index on a global scale. *Journal of Hydrology*, *212–213*, 268–286. [https://doi.org/10.1016/S0022-1694\(98\)00211-X](https://doi.org/10.1016/S0022-1694(98)00211-X)
- Kergoat, L. (2002). Impact of doubled CO<sub>2</sub> on global-scale leaf area index and evapotranspiration: Conflicting stomatal conductance and LAI responses. *Journal of Geophysical Research*, *107*(D24), 4808. <https://doi.org/10.1029/2001JD001245>
- Knauer, J., Zaehle, S., Reichstein, M., Medlyn, B. E., Forkel, M., Hagemann, S., & Werner, C. (2017). The response of ecosystem water-use efficiency to rising atmospheric CO<sub>2</sub> concentrations: Sensitivity and large-scale biogeochemical implications. *The New Phytologist*, *213*(4), 1654–1666. <https://doi.org/10.1111/nph.14288>
- Knyazikhin, Y., Myneni, R. B., Privette, J. L., Running, S. W., Nemani, R., Zhang, Y., et al. (1999). MODIS Leaf Area Index (LAI) and Fraction of Photosynthetically Active Radiation absorbed by vegetation (FPAR) Product (MOD15) Algorithm Theoretical Basis Document, Version 4. (4.0), 130. <http://eosps0.gsfc.nasa.gov/atbd/modistables.html>
- Kool, D., Agam, N., Lazarovitch, N., Heitman, J. L., Sauer, T. J., & Ben-Gal, A. (2014). A review of approaches for evapotranspiration partitioning. *Agricultural and Forest Meteorology*, *184*, 56–70. <https://doi.org/10.1016/j.agrformet.2013.09.003>
- Liddell, M., & Laurance, S. (2015). Leaf area index data, Far North Queensland Rainforest SuperSite, Daintree Rainforest Observatory, Cape Tribulation, Core 1ha, 2014. TERN Australian SuperSite Network. <http://www.supersites.net.au/knb/metacat/supersite.238.12/html>. Accessed on 1/11/2017.
- Lin, Y.-S., Medlyn, B. E., Duursma, R. A., Prentice, I. C., Wang, H., Baig, S., et al. (2015). Optimal stomatal behaviour around the world. *Nature Climate Change*, *5*(5), 459–464. <https://doi.org/10.1038/nclimate2550>
- Liu, B., Guan, H., Zhao, W., Yang, Y., & Li, S. (2017). Groundwater facilitated water-use efficiency along a gradient of groundwater depth in arid northwestern China. *Agricultural and Forest Meteorology*, *233*, 235–241. <https://doi.org/10.1016/j.agrformet.2016.12.003>
- Lu, Y., Duursma, R. A., & Medlyn, B. E. (2016). Optimal stomatal behaviour under stochastic rainfall. *Journal of Theoretical Biology*, *394*, 160–171. <https://doi.org/10.1016/j.jtbi.2016.01.003>
- Mahowald, N., Lo, F., Zheng, Y., Harrison, L., Funk, C., Lombardozzi, D., & Goodale, C. (2016). Projections of leaf area index in Earth system models. *Earth System Dynamics*, *7*(1), 211–229. <https://doi.org/10.5194/esd-7-211-2016>
- Manzoni, S., Vico, G., Palmroth, S., Porporato, A., & Katul, G. (2013). Optimization of stomatal conductance for maximum carbon gain under dynamic soil moisture. *Advances in Water Resources*, *62*, 90–105. <https://doi.org/10.1016/j.advwatres.2013.09.020>
- McMurtrie, R. E., & Dewar, R. C. (2013). New insights into carbon allocation by trees from the hypothesis that annual wood production is maximized. *The New Phytologist*, *199*(4), 981–990. <https://doi.org/10.1111/nph.12344>
- McMurtrie, R. E., Norby, R. J., Medlyn, B. E., Dewar, R. C., Pepper, D. A., Reich, P. B., & Barton, C. V. M. (2008). Why is plant-growth response to elevated CO<sub>2</sub> amplified when water is limiting, but reduced when nitrogen is limiting? A growth-optimisation hypothesis. *Functional Plant Biology*, *35*(6), 521–534. <https://doi.org/10.1071/FP08128>
- Medlyn, B. E., Barton, C. V. M., Broadmeadow, M. S. J., Ceulemans, R., De Angelis, P., Forstreuter, M., et al. (2001). Stomatal conductance of forest species after long-term exposure to elevated CO<sub>2</sub> concentration: A synthesis. *The New Phytologist*, *149*(2), 247–264. <https://doi.org/10.1046/j.1469-8137.2001.00028.x>
- Medlyn, B. E., de Kauwe, M. G., Lin, Y. S., Knauer, J., Duursma, R. A., Williams, C. A., et al. (2017). How do leaf and ecosystem measures of water-use efficiency compare? *The New Phytologist*, *216*(3), 758–770. <https://doi.org/10.1111/nph.14626>
- Medlyn, B. E., de Kauwe, M. G., Zaehle, S., Walker, A. P., Duursma, R. A., Luus, K., et al. (2016). Using models to guide field experiments: A priori predictions for the CO<sub>2</sub> response of a nutrient- and water-limited native eucalyptus woodland. *Plant, Cell and Environment*, *22*(8), 2834–2851. <https://doi.org/10.1111/gcb.13268>
- Medlyn, B. E., Dreyer, E., Ellsworth, D., Forstreuter, M., Harley, P. C., Kirschbaum, M. U. F., et al. (2002). Temperature response of parameters of a biochemically based model of photosynthesis. II. A review of experimental data. *Plant, Cell and Environment*, *25*(9), 1167–1179. <https://doi.org/10.1046/j.1365-3040.2002.00891.x>
- Medlyn, B. E., Duursma, R. A., Eamus, D., Ellsworth, D. S., Prentice, I. C., Barton, C. V. M., et al. (2011). Reconciling the optimal and empirical approaches to modelling stomatal conductance. *Global Change Biology*, *17*(6), 2134–2144. <https://doi.org/10.1111/j.1365-2486.2010.02375.x>
- Medlyn, B. E., Pepper, D. A., O'Grady, A. P., & Keith, H. (2007). Linking leaf and tree water use with an individual-tree model. *Tree Physiology*, *27*(12), 1687–1699. <https://doi.org/10.1093/treephys/27.12.1687>
- Mehran, A., AghaKouchak, A., & Phillips, T. J. (2014). Evaluation of CMIP5 continental precipitation simulations relative to satellite-based gauge-adjusted observations. *Journal of Geophysical Research: Atmospheres*, *119*, 1695–1707. <https://doi.org/10.1002/2013JD021152>
- Méndez-Toribio, M. G., Ibarra-Manríquez, G., Navarrete-Segueda, A., & Paz, H. (2017). Topographic position, but not slope aspect, drives the dominance of functional strategies of tropical dry forest trees. *Environmental Research Letters*, *12*(8), 85002. <https://doi.org/10.1088/1748-9326/aa717b>
- Mitchell, P. J., Veneklaas, E., Lambers, H., & Burgess, S. S. O. (2009). Partitioning of evapotranspiration in a semi-arid eucalypt woodland in south-western Australia. *Agricultural and Forest Meteorology*, *149*(1), 25–37. <https://doi.org/10.1016/j.agrformet.2008.07.008>
- Murray-Tortarolo, G., Anav, A., Friedlingstein, P., Sitch, S., Piao, S., Zhu, Z., et al. (2013). Evaluation of land surface models in reproducing satellite-derived LAI over the high-latitude northern hemisphere. Part I: Uncoupled DGVMs. *Remote Sensing*, *5*(10), 4819–4838. <https://doi.org/10.3390/rs5104819>
- Nemani, R. R., & Running, S. W. (1989). Testing a theoretical climate-soil-leaf area hydrologic equilibrium of forests using satellite data and ecosystem simulation. *Agricultural and Forest Meteorology*, *44*(3–4), 245–260. [https://doi.org/10.1016/0168-1923\(89\)90020-8](https://doi.org/10.1016/0168-1923(89)90020-8)
- Norby, R., Gu, L., Haworth, I. C., Jensen, A. M., Turner, B. L., Walker, A. P., et al. (2017). Informing models through empirical relationships between foliar phosphorus, nitrogen and photosynthesis across diverse woody species in tropical forests of Panama. *The New Phytologist*, *215*(4), 1425–1437. <https://doi.org/10.1111/nph.14319>
- Onoda, Y., Wright, I. J., Evans, J. R., Hikosaka, K., Kitajima, K., Niinemets, Ü., et al. (2017). Physiological and structural tradeoffs underlying the leaf economics spectrum. *The New Phytologist*, *214*(4), 1447–1463. <https://doi.org/10.1111/nph.14496>
- Paget, M. J., & King, E. A. (2008). MODIS Land data sets for the Australian region. CSIRO Marine and Atmospheric Research Internal Report 004. <http://remote-sensing.nci.org.au/u39/public/html/modis/lpdaac-mosaics-cmar/> Land Processes Distributed Active Archive Center (LPDAAC). <http://lpdaac.usgs.gov>
- Pappas, C., Faticchi, S., & Burlando, P. (2016). Modeling terrestrial carbon and water dynamics across climatic gradients: Does plant trait diversity matter? *The New Phytologist*, *209*(1), 137–151. <https://doi.org/10.1111/nph.13590>

- Prentice, I. C., Dong, N., Gleason, S. M., Maire, V., & Wright, I. J. (2014). Balancing the costs of carbon gain and water transport: testing a new theoretical framework for plant functional ecology. *Ecology Letters*, *17*(1), 82–91. <https://doi.org/10.1111/ele.12211>
- Prober, S., & Macfarlane, C. (2013). Leaf area index and cover of four 1 ha plots, Great Western Woodlands SuperSite, 2015. TERN Australian SuperSite Network. Retrieved from <http://supersites.tern.org.au/knb/metacat/supersite.304.6/html>, Accessed on 1/11/2017.
- Prober, S., & Macfarlane, C. (2015). Leaf area index and cover of four 1 ha plots, Great Western Woodlands SuperSite, 2015. TERN Australian SuperSite Network. <http://supersites.tern.org.au/knb/metacat/supersite.304.6/html>. Accessed on 1/11/2017.
- Reich, P. B., Sendall, K. M., Stefanski, A., Wei, X., Rich, R. L., & Montgomery, R. A. (2016). Boreal and temperate trees show strong acclimation of respiration to warming. *Nature*, *531*(7596), 633–636. <https://doi.org/10.1038/nature17142>
- Rowlings, D., & Grace, P. (2015). Leaf area index data, south-east Queensland Peri-urban SuperSite, Samford, Core 1 ha, 2015. TERN Australian SuperSite Network. <http://www.supersites.net.au/knb/metacat/supersite.284.6/html>. Accessed on 1/11/2017.
- Ryan, M. G. (1991). A simple method for estimating gross carbon budgets for vegetation in forest ecosystems. *Tree Physiology*, *9*(12), 255–266. <https://doi.org/10.1093/treephys/9.1-2.255>
- Sands, P. J. (1995). Modelling canopy production. 11. From single-leaf photosynthetic parameters to daily canopy photosynthesis. *Australian Journal of Plant Physiology*, *22*(4), 603–614. <https://doi.org/10.1071/PP9950603>
- Sands, P. J. (1996). Modelling canopy production. III. Canopy light-utilisation efficiency and its sensitivity to physiological and environmental variables. *Functional Plant Biology*, *23*(1), 103–114. <https://doi.org/10.1071/PP9960103>
- Schymanski, S. J., Roderick, M. L., & Sivapalan, M. (2015). Using an optimality model to understand medium and long-term responses of vegetation water use to elevated atmospheric CO<sub>2</sub> concentrations. *AoB Plants*, *7*(1), plv060. <https://doi.org/10.1093/aobpla/plv060>
- Smith, N. G., Malyshev, S. L., Shevliakova, E., Kattge, J., & Dukes, J. S. (2015). Foliar temperature acclimation reduces simulated carbon sensitivity to climate. *Nature Climate Change*, *6*, 407–411. <https://doi.org/10.1038/nclimate2878>
- Specht, R. L., & Specht, A. (1989). Canopy structure in Eucalyptus-dominated communities in Australia along climatic gradients. *Acta Oecologica Oecologia Plant*, *10*(2), 191–213.
- Sutanto, S. J., Wenninger, J., Coenders-Gerrits, A. M. J., & Uhlenbrook, S. (2012). Partitioning of evaporation into transpiration, soil evaporation and interception: A comparison between isotope measurements and a HYDRUS-1D model. *Hydrology and Earth System Sciences*, *16*(8), 2605–2616. <https://doi.org/10.5194/hess-16-2605-2012>
- van Gorsel, E. (2015). Leaf area index data, Tumbarumba Wet Eucalypt SuperSite, 2014. TERN Australian SuperSite Network. <http://www.supersites.net.au/knb/metacat/supersite.297.5/html>. Accessed on 1/11/2017.
- Villar, R., & Merino, J. (2001). Comparison of leaf construction costs in woody species with differing leaf life-spans in contrasting ecosystems. *The New Phytologist*, *151*(1), 213–226. <https://doi.org/10.1046/j.1469-8137.2001.00147.x>
- Viscarra Rossel, R., Chen, C., Grundy, M., Searle, S., Clifford, D., Odgers, N., et al. (2014a). Soil and landscape grid national soil attribute maps—Nitrogen (3° resolution)—Release 1. v4, CSIRO, data collection. <https://doi.org/10.4225/08/546F564AE11F9>
- Viscarra Rossel, R., Chen, C., Grundy, M., Searle, S., Clifford, D., Odgers, N., et al. (2014b). Soil and landscape grid national soil attribute maps—Total phosphorus (3° resolution)—Release 1. v4, CSIRO, data collection. <https://doi.org/10.4225/08/546F617719CAF>
- Walker, A. P., Hanson, P. J., De Kauwe, M. G., Medlyn, B. E., Zaehle, S., Asao, S., et al. (2014). Comprehensive ecosystem model-data synthesis using multiple data sets at two temperate forest free-air CO<sub>2</sub> enrichment experiments, Model performance at *Journal of Geophysical Research: Biogeosciences*, *119*, 937–964. <https://doi.org/10.1002/2013JG002553>
- Wang, K., & Dickinson, R. E. (2012). A review of global terrestrial evapotranspiration: Observation, modelling, climatology, and climatic variability. *Reviews of Geophysics*, *50*(2011), 1–54. <https://doi.org/10.1029/2011RG000373.1>
- Wang, L., Caylor, K. K., Villegas, J. C., Barron-Gafford, G. A., Breshears, D. D., & Huxman, T. E. (2010). Partitioning evapotranspiration across gradients of woody plant cover: Assessment of a stable isotope technique. *Geophysical Research Letters*, *37*, L09401. <https://doi.org/10.1029/2010GL043228>
- Wang, L., Good, S. P., & Caylor, K. K. (2014). Global synthesis of vegetation control on evapotranspiration partitioning. *Geophysical Research Letters*, *41*, 6753–6757. <https://doi.org/10.1002/2014GL061439>
- Whitley, R., Evans, B., Pauwels, J., Hutchinson, M., Xu, T., Han, W., et al. (2014). Actual evapotranspiration (approximated), actual vapor pressure, annual mean radiation, annual precipitation, monthly maximum temperature: eMAST-R-Package 2.0, 0.01 degree, Australian coverage, 1970–2012, Macquarie University, Sydney, Australia. Obtained from <http://dap.nci.org.au>, made available by the Ecosystem Modelling and Scaling Infrastructure (eMAST, <http://www.emast.org.au>) Facility of the Terrestrial Ecosystem Research Network (TERN, <http://www.tern.org.au>). Accessed (2016–05-05).
- Wild, A. (1958). The phosphate content of Australian soils. *Australian Journal of Agricultural Research*, *9*(2), 193–204. <https://doi.org/10.1071/AR9580193>
- Wolf, A., Anderegg, W. R. L., & Pacala, S. W. (2016). Optimal stomatal behavior with competition for water and risk of hydraulic impairment. *Proceedings of the National Academy of Sciences of the United States of America*, *113*(46), E7222–E7230. <https://doi.org/10.1073/pnas.1615144113>
- Woodward, F. I. (1987). Climate and plant distribution. *Cambridge Press*, *154*(2), 272. <https://doi.org/10.2307/633873>
- Woodward, F. I., & Lomas, M. R. (2004). Vegetation dynamics—Simulating responses to climatic change. *Biological Reviews of the Cambridge Philosophical Society*, *79*(3), 643–670. <https://doi.org/10.1017/s1464793103006419>
- Wright, I. J., Reich, P. B., Westoby, M., Ackerly, D. D., Baruch, Z., Bongers, F., et al. (2004). The worldwide leaf economics spectrum. *Nature*, *428*(6985), 821–827. <https://doi.org/10.1038/nature02403>
- Xu, X., Medvigy, D., Joseph Wright, S., Kitajima, K., Wu, J., Albert, L. P., et al. (2017). Variations of leaf longevity in tropical moist forests predicted by a trait-driven carbon optimality model. *Ecology Letters*, *20*(9), 1097–1106. <https://doi.org/10.1111/ele.12804>
- Yang, Y., Donohue, R. J., McVicar, T. R., Roderick, M. L., & Beck, H. E. (2016). Long-term CO<sub>2</sub> fertilization increases vegetation productivity and has little effect on hydrological partitioning in tropical rainforests. *Journal of Geophysical Research: Biogeosciences*, *121*, 2125–2140. <https://doi.org/10.1002/2016JG003475>
- Yepez, E. A., Huxman, T. E., Ignace, D. D., English, N. B., Weltzin, J. F., Castellanos, A. E., & Williams, D. G. (2005). Dynamics of transpiration and evaporation following a moisture pulse in semiarid grassland: A chamber-based isotope method for partitioning flux components. *Agricultural and Forest Meteorology*, *132*(3–4), 359–376. <https://doi.org/10.1016/j.agrformet.2005.09.006>
- Zeppel, M. C., Macinnis-Ng, C., Palmer, A., Taylor, D., Whitley, R., Fuentes, S., et al. (2008). An analysis of the sensitivity of sap flux to soil and plant variables assessed for an Australian woodland using a soil-plant-atmosphere model. *Functional Plant Biology*, *35*(6), 509–520. <https://doi.org/10.1071/FP08114>
- Zhang, L., Dawes, W. R., & Walker, G. R. (2001). Response of mean annual evapotranspiration to vegetation changes at catchment scale. *Water Resources*, *37*(3), 701–708.